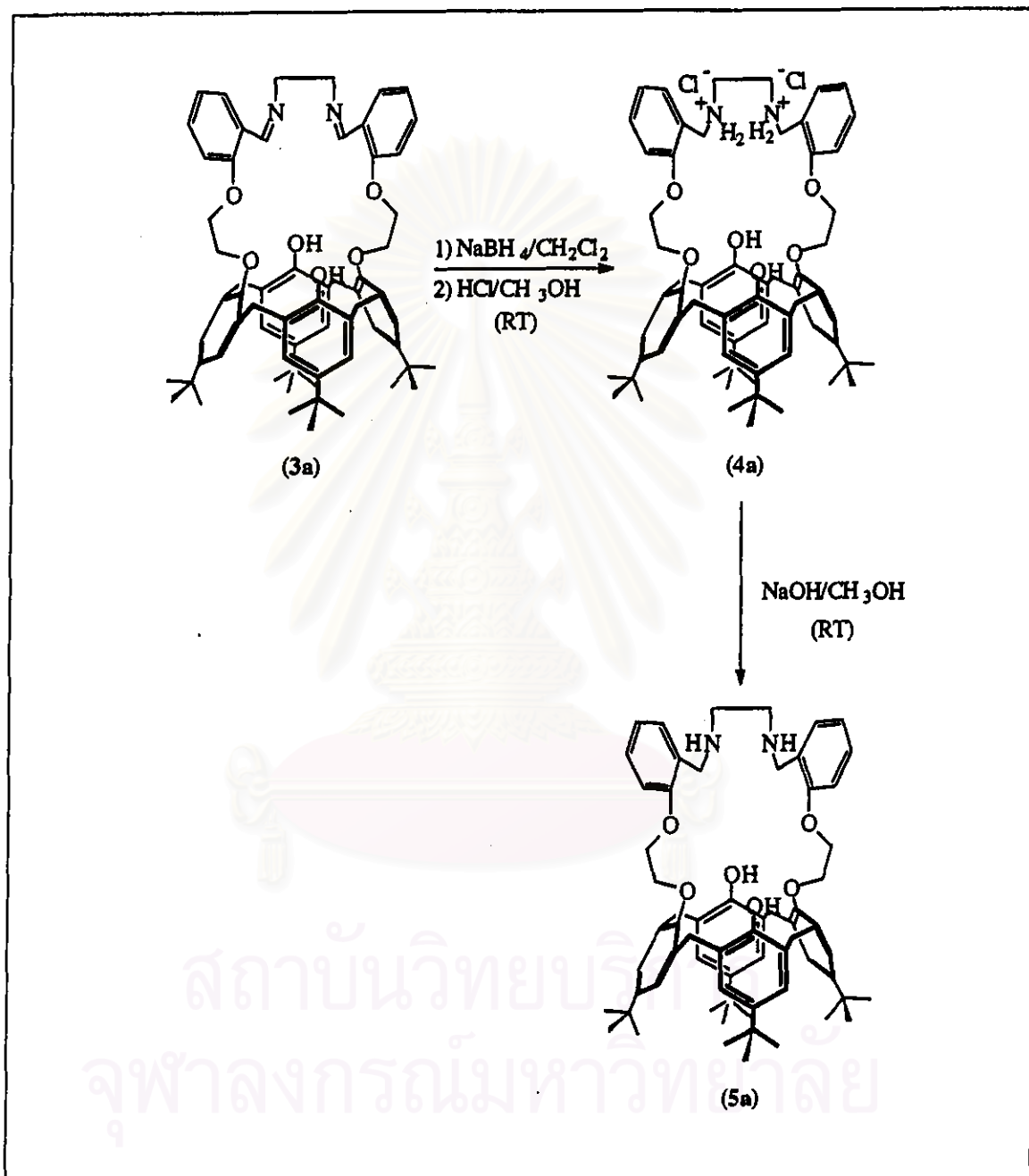


## CHAPTER III

### RESULTS AND DISCUSSION

#### 3.1 Synthesis and Characterization of Calix[4]arene Derivatives

The construction of diaza benzo crown ether *p*-*tert*-butylcalix[4]arene (5a) is achieved via the initial synthesis of the protonated product (4a) (Scheme 3.1). The ligand (4a) is prepared by reducing the Schiff's base diaza benzo crown ether *p*-*tert*-butylcalix[4]arene (3a)<sup>23</sup> with NaBH<sub>4</sub> and then protonating with HCl/CH<sub>3</sub>OH to afford the hydrogen chloride product in 83%. The formation of the ligand (4a) is indicated by the arising of the signal of ammonium protons (NH<sub>2</sub><sup>+</sup>Cl<sup>-</sup>-CH<sub>2</sub>) at 9.87 ppm in place of the imine protons (-HC=N-CH<sub>2</sub>-) at 9.02 ppm (Figure 3.1). The neutral form, ligand (5a), was obtained in 66% after neutralizing ligand (4a) with sodium hydroxide in methanol. The protons beside nitrogen centers in ligand (5a) (3.89 and 2.59 ppm for Ar-CH<sub>2</sub>-NH and N-CH<sub>2</sub>-CH<sub>2</sub>, respectively) shifted to higher field relative to those of the ligand (4a) (4.51 and 3.76 ppm for Ar-CH<sub>2</sub>-NH and N-CH<sub>2</sub>-CH<sub>2</sub>, respectively) owing to disappearance of the positive charge (Figure 3.1).



**Scheme 3.1** The procedure for preparation of ligand (5a)

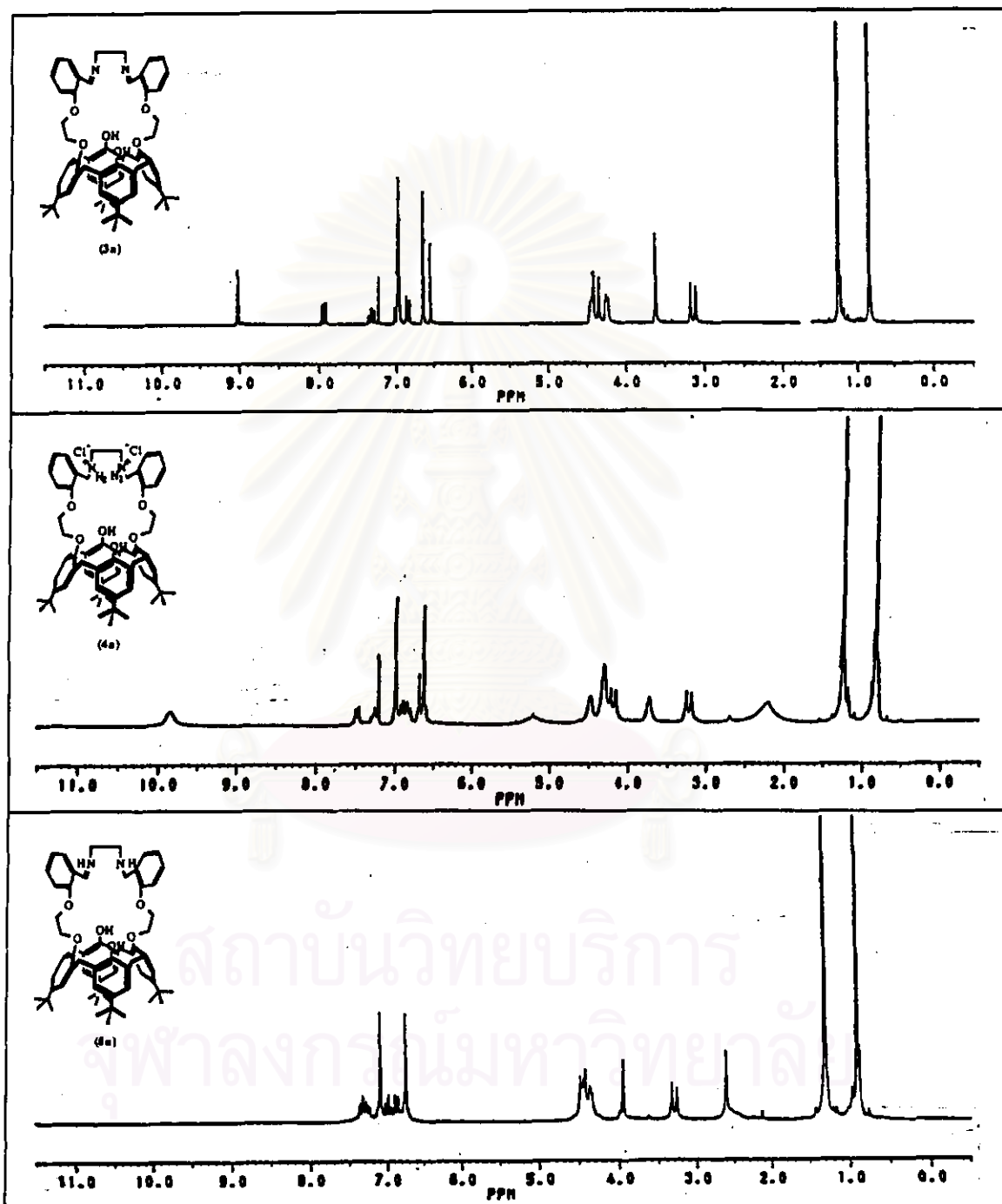
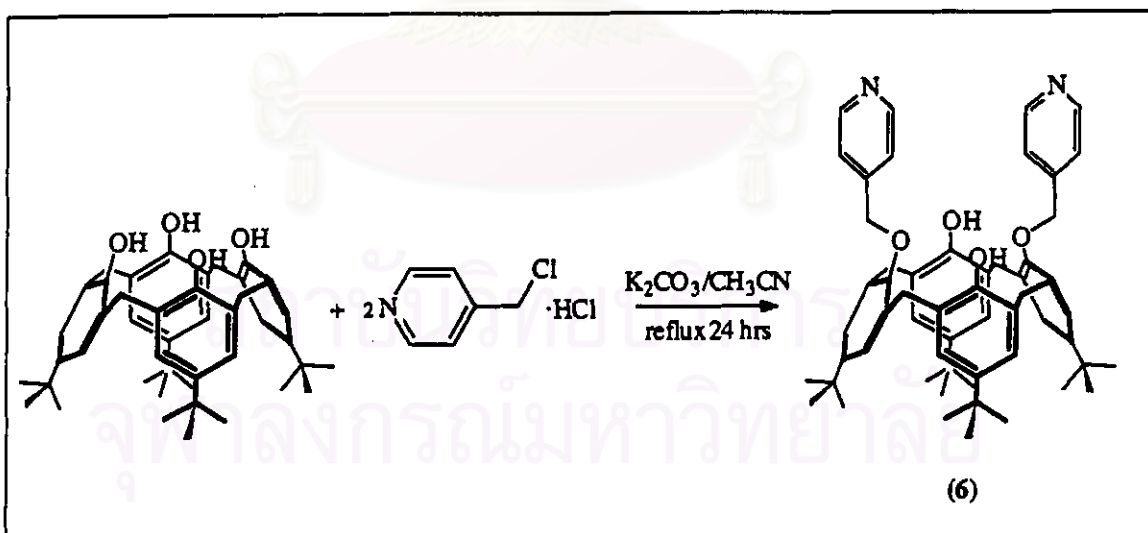
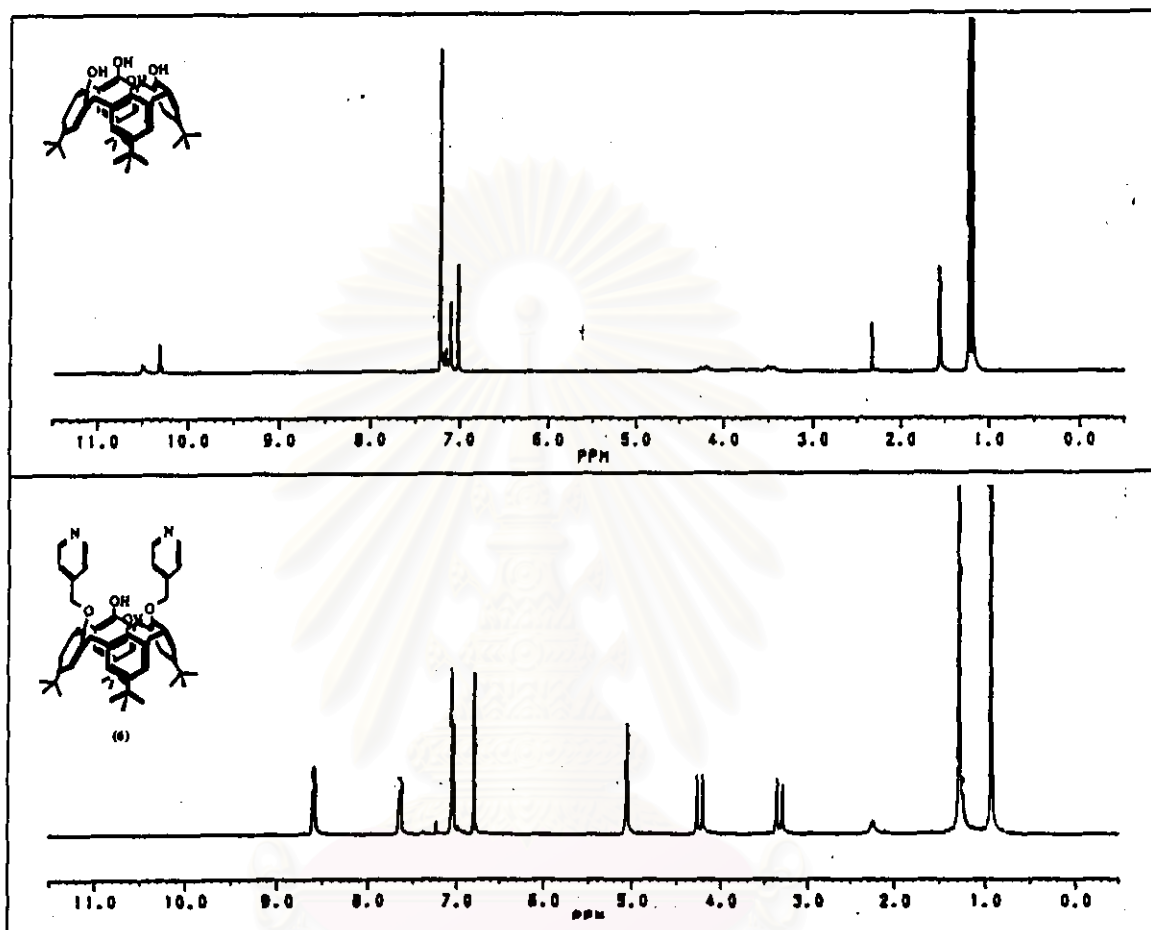


Figure 3.1.  $^1\text{H-NMR}$  spectra of ligands (3a), (4a) and (5a).

Another *p-tert*-butyl calix[4]arene derivative, 25,27-di-(4-pyridylmethoxy)-*p-tert*-butylcalix[4]arene (**6**) was synthesized by alkylating calix[4]arene with two equivalents of 4-(chloromethyl)pyridine hydrochloride in acetonitrile in the presence of  $K_2CO_3$  as base and small amount of NaI (5 equivalence) as catalyst (Scheme 3.2). Separation of the products by column chromatography ( $SiO_2$ ) using 10% acetone in dichloromethane as eluent gave ligand (**6**) in 44 % yield. Compared to other pyridylmethoxy derivatives such as *ortho*-<sup>28</sup> and *meta*<sup>29</sup> derivatives, the *para* derivative (**6**) was obtained in lower yield because the N-donor in a *para* position could not chelate the  $K^+$  ion for stabilizing the phenoxide anion and for preorganizing the pyridyl group to facilitate the nucleophilic substitution reaction. The  $^1H$ -NMR spectrum of ligand (**6**) composed of a singlet signal of Ar-OCH<sub>2</sub>-Py at 5.05 ppm and two doublets of the aromatic protons on the pyridine moieties at 8.60 and 7.64 ppm as well as the signals of the *p-tert*-butyl calix[4]arene moiety (Figure 3.2).



Scheme 3.2 The procedure for preparation of ligand (**6**)



**Figure 3.2.**  $^1\text{H-NMR}$  spectrum of *p-tert-butylcalix[4]arene* and ligand (6).

Ligands (3a)-(5a) and (6) orientate in cone conformation indicated by doublet of doublet signals<sup>30</sup> between 3.1–4.4 ppm due to the methylene bridged protons on the lower rim with a coupling constant of  $\sim 13$  Hz. Moreover, the  $^{13}\text{C-NMR}$  spectrum, elemental analysis and MALDI-TOF-MS also supported the identity of ligands (5a) and (6).



3.6 respectively. Unfortunately, the plots indicated that ligands (5a)–(5c) could not form complexes with the aforementioned anions.

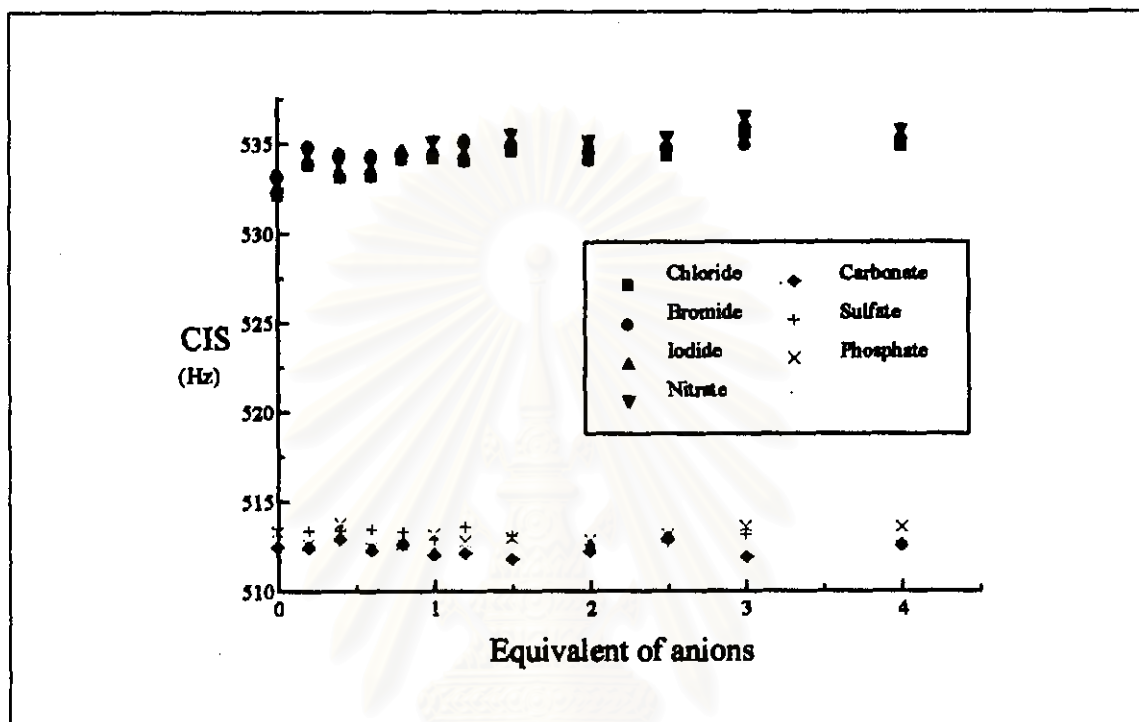


Figure 3.4. Plot of CIS versus equivalent of various anions added for ligand (5a).

สถาบันวิทยบริการ  
จุฬาลงกรณ์มหาวิทยาลัย

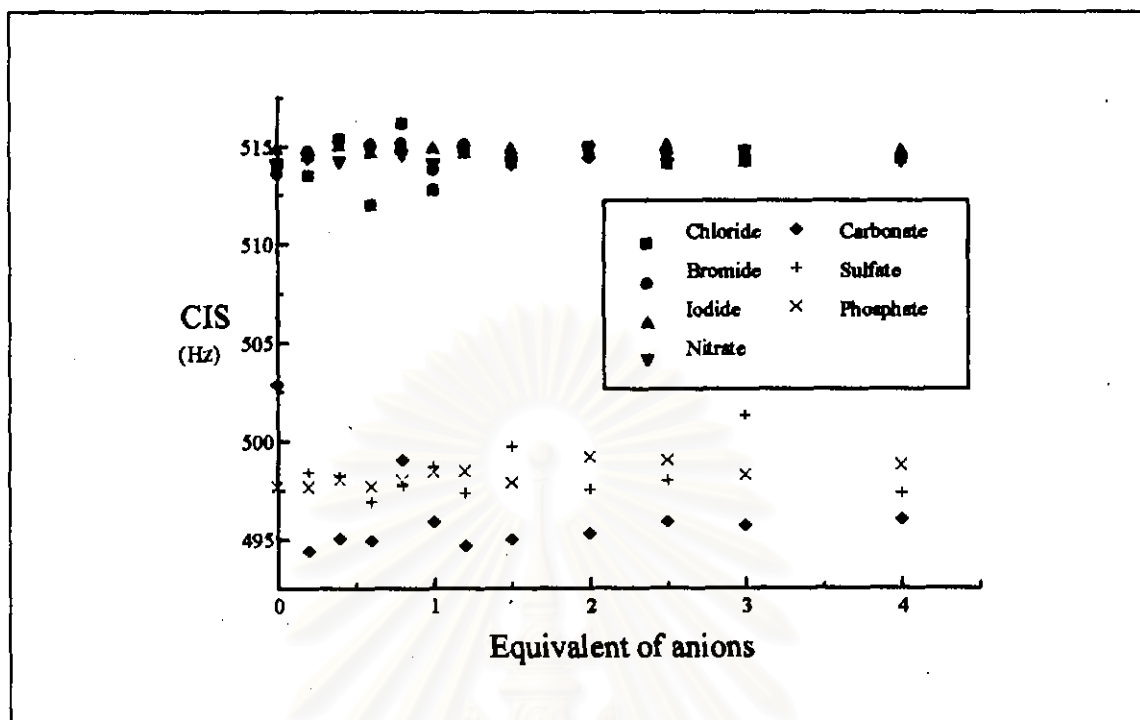


Figure 3.5. Plot of CIS versus equivalent of various anions added for ligand (5b).

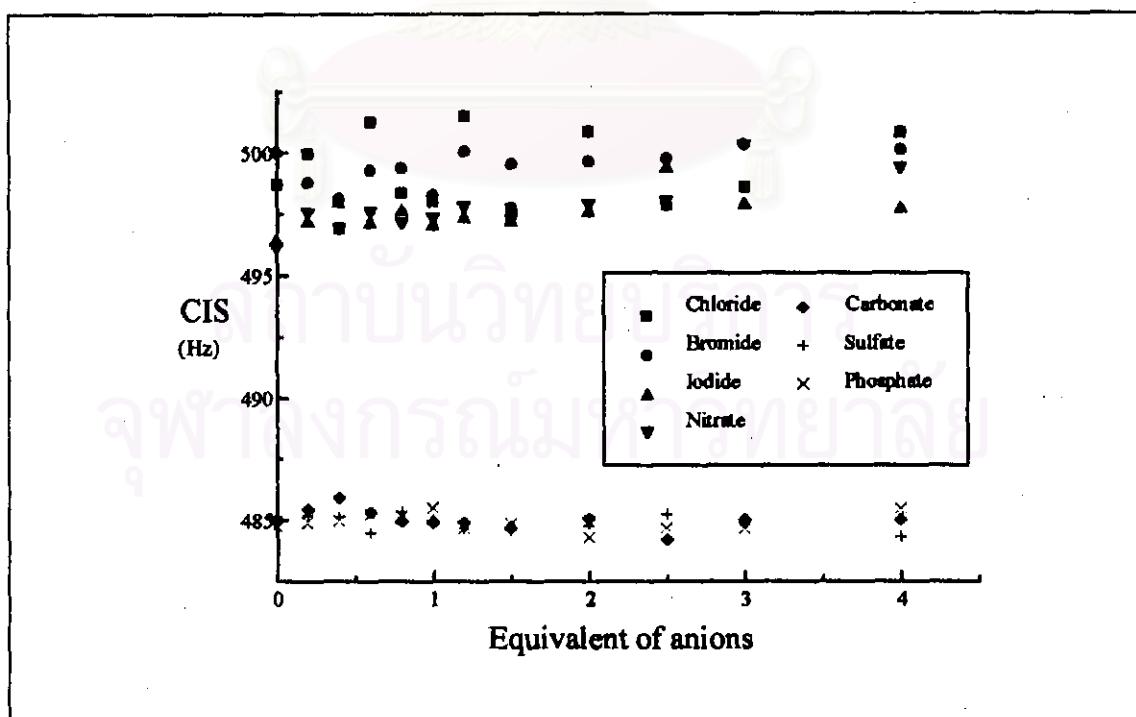


Figure 3.6. Plot of CIS versus equivalent of various anions added for ligand (5c).



These negative results may stem from the repulsion between the lone pair electron of the amine group in these receptors and the charge of anions. In the literature<sup>31-35</sup>, the neutral receptor that bound anions contained electron withdrawing group such as carbonyl or sulfonyl attached to amine nitrogen atoms. The anion size may also be too large to include in the amine cavity of the receptor, and the hydrogen bonding may be too weak to hold the guests outside the cavity of the molecules.

### 3.2.2 Neutral Complexation

Analogous <sup>1</sup>H-NMR titrations were also used to investigate host-guest chemistry of ligand (6) towards neutral molecules *via* hydrogen bonding interaction. A series of compounds containing hydrogen bond donors such as 1,3-dialdehyde crown-*p-tert*-butyl calix[4]arene (ligands (2-1) and (2-2), Figure 3.7), 1,2-diaminoethane, 2,6-diaminopyridine, 1,2-dihydroxybenzene (catechol), 1,3-dihydroxybenzene (resorcinol), 1,4-dihydroxybenzene (hydroquinone), benzene-1,2-dicarboxylic acid (phthalic acid), benzene-1,3-dicarboxylic acid (isophthalic acid) and benzene-1,4-dicarboxylic acid (terephthalic acid) were used in the investigation.

สถาบันวิทยบริการ  
จุฬาลงกรณ์มหาวิทยาลัย

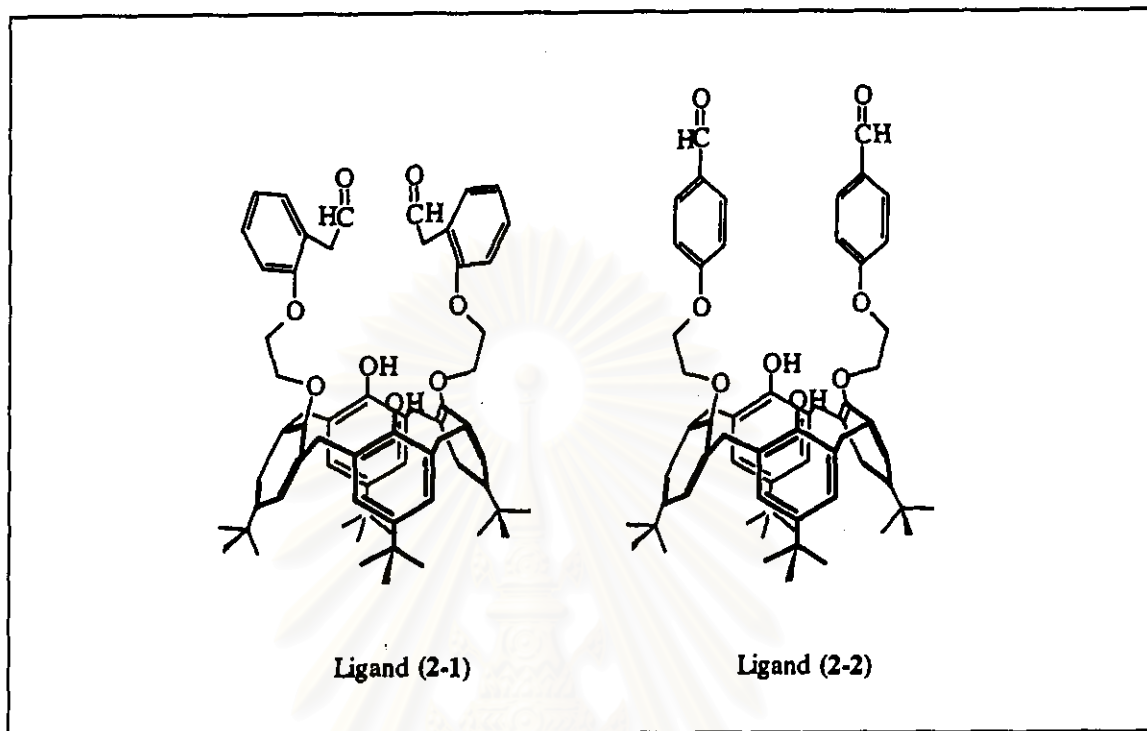


**Figure 3.7.** Structures of ligand (2-1) and (2-2).

In addition, 2,4-pentanedione or acetylacetone has also been used in hydrogen bonding investigation of ligand (6). Generally, 2,4-pentanedione occurs in solution as an equilibrium mixture of 87% enol and 13% diketone<sup>36</sup>. The keto form contains acidic methylene protons which are suitable for hydrogen bonding with ligand (6). The change in a keto:enol proportion due to hydrogen bonding interaction is expected to be observed.

<sup>1</sup>H-NMR titrations of ligand (6) with various hydrogen bond donors were performed in CDCl<sub>3</sub> solution. The results depicted in Figure 3.8 show that the proton on the *ortho* position of the pyridine (Py-2-proton) only slightly shifted upon addition of hydrogen bond donors and suggest that ligand (6) has no recognition towards ligands (2-1) and (2-2), 1,2-diaminoethane, 2,6-diaminopyridine, acetylacetone, hydroquinone, isophthalic acid and terephthalic acid. The dialdehyde derivative of calixarenes, (2-1) and (2-2), are weak hydrogen bond donors<sup>37</sup>. The hydrogen

bonding interaction may thus be too weak to be observed by NMR spectroscopy. For moderate hydrogen bond donors, 1,2-diaminoethane and 2,6-diaminopyridine, the absence of hydrogen bonding interaction with ligand (6) may stem from the electron repulsion between N-amine and N-pyridine. Thus, the amine group should be attached an electron withdrawing group to increase the ability of hydrogen bonding<sup>38</sup>. It is fascinating that no hydrogen bonding between ligand (6) and acetylacetone has been observed. The intramolecular hydrogen bonding between -O-H and O=C- in the enol form must be very strong and prevents the intermolecular hydrogen bonding to occur.

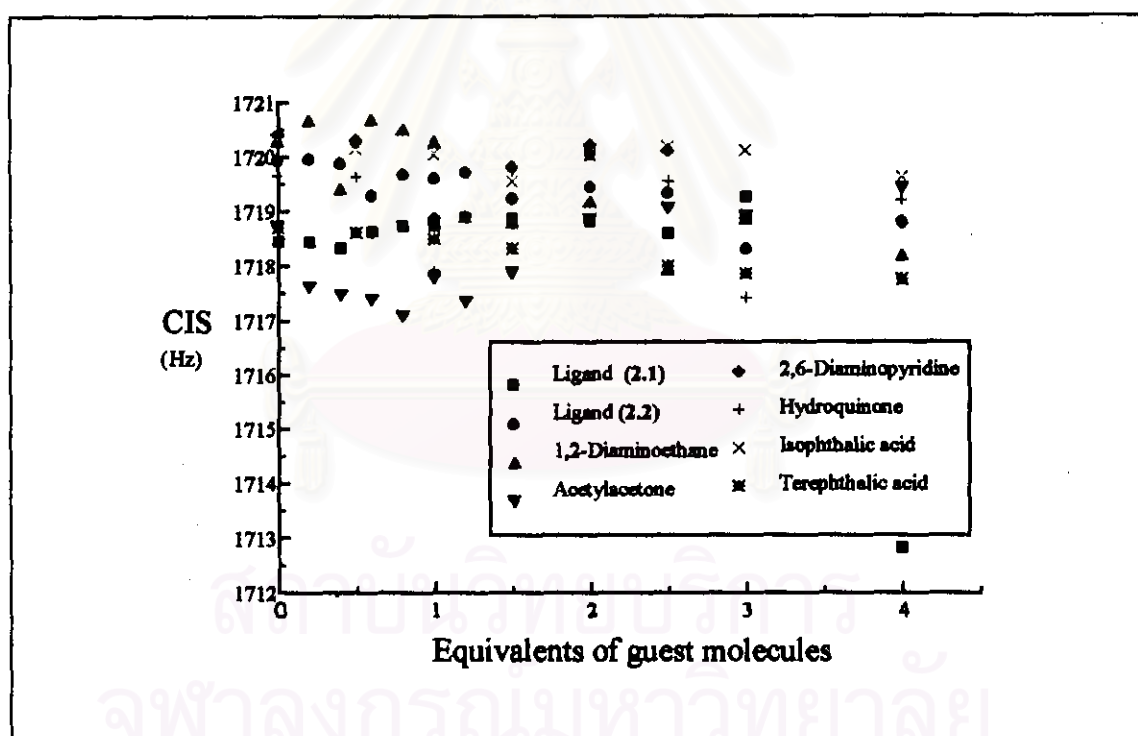


**Figure 3.8.** Plot of CIS versus equivalents of various hydrogen bond donors.

### 3.2.2.1 Complexation Studies of Dihydroxybenzene

Complexation studies of dihydroxybenzenes contained two hydroxy groups at different positions as hydrogen bond donor with ligand (6) are performed by adding various amounts of the guests into a deuterated chloroform solution of the host (6) and investigated the interaction by  $^1\text{H-NMR}$  spectroscopy. Due to the insolubility of dihydroxybenzenes except catechol<sup>39</sup>, they were added directly as solid into NMR tubes. Dissolution of the solids into the solution of ligand (6) also indicates that the inclusion of alcohols by ligand (6) has occurred. It was found that ligand (6) could not dissolve hydroquinone, and the Py-2-proton only slightly shifted as shown in Figure 3.8. Only binding ability of the receptor towards catechol and resorcinol can be determined.

#### 3.2.2.1.1 Complexation Studies of 1,3-Dihydroxybenzene (Resorcinol)

A typical  $^1\text{H-NMR}$  spectrum of the complexation studies between ligand (6) and resorcinol is shown in Figure 3.9. The addition of 1,3-dihydroxybenzene into deuterated chloroform solution of ligand (6) leads to the evolution of a new set of proton resonances at 7.13 (t), 6.59 (d) and 6.46 (dd) ppm. All signals except Py-2-proton shifted continuously downfield until 1 equivalent of the guest had been added (Figure 3.10). The signal movement can be attributed to hydrogen bonding interaction, magnetic anisotropy<sup>40-41</sup> and reorganization of the structure of ligand (6), *vide infra*. Nevertheless, each  $^1\text{H-NMR}$  spectrum possesses a doublet of doublet signal at  $\sim 3.34$  and  $\sim 4.23$  ppm ( $J \sim 13$  Hz) suggesting that ligand (6) retains the cone conformation of calix[4]arene upon complexation.

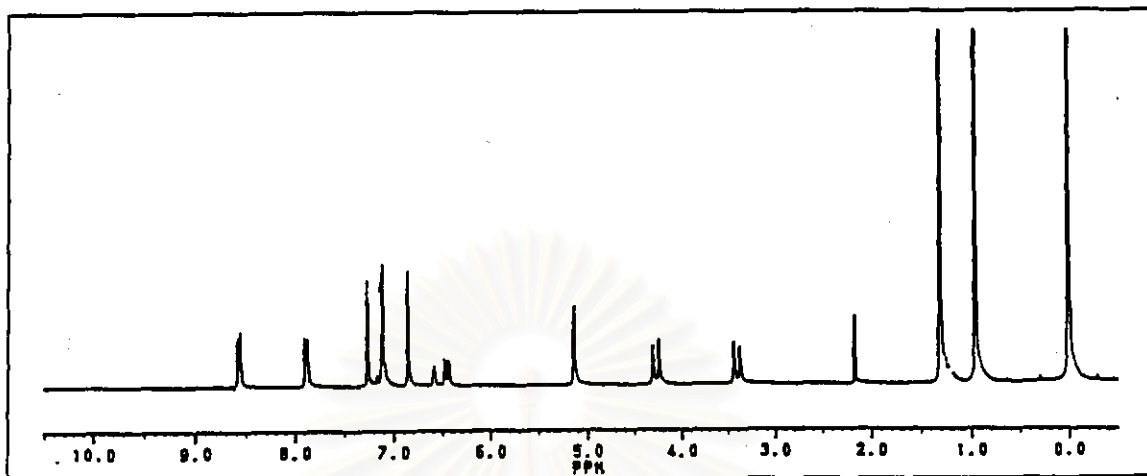


**Figure 3.9.** A  $^1\text{H}$ -NMR spectrum of the complexation studies between ligand (6) and resorcinol.

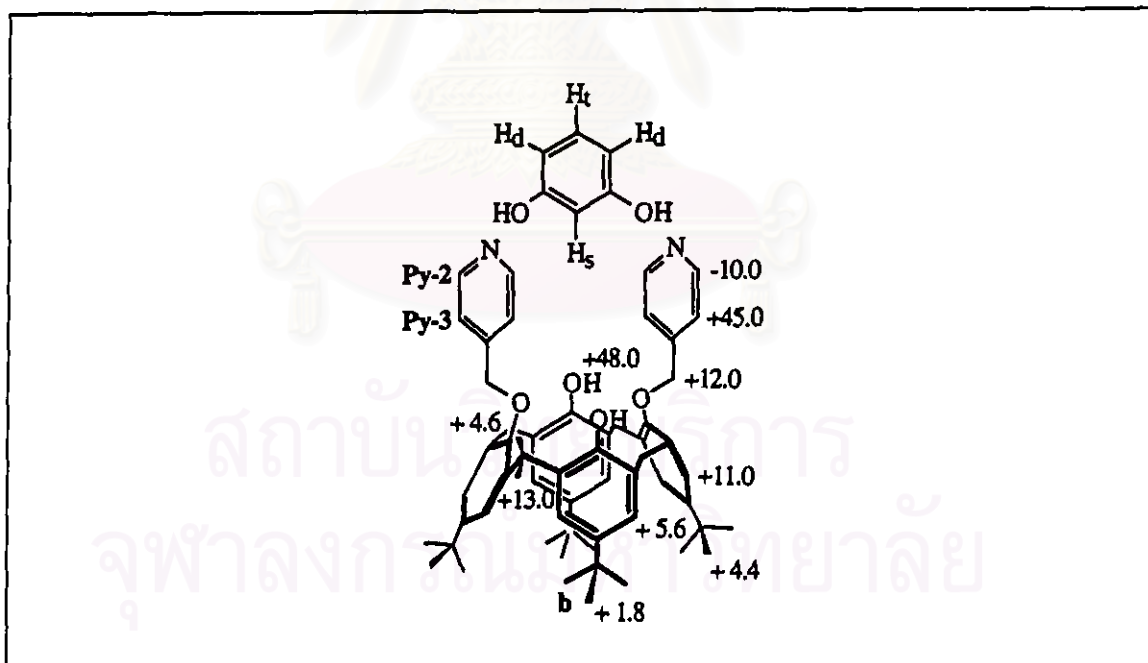


**Figure 3.10.** The complexation induced shift (CIS ( $\Delta\delta$  (Hz))) referred to  $\text{CDCl}_3$  of all protons on ligand (6) when adding 1 equivalent of resorcinol ((+) represents downfield shift and (-) represents upfield shift).

The CIS of Py-2-proton, Py-3-proton and hydroxy proton ( $ArOH$ ) are collected in Table 3.2. A plot of CIS against the equivalent of 1,3-dihydroxybenzene is displayed in Figure 3.11. The plot suggests that ligand (6) forms a complex with resorcinol in a 1:1 fashion. The stability or complex formation constant of ligand (6) towards resorcinol can then be estimated from the data in Table 3.1 using a curve-fitting program. It is found that ligand (6) forms a very strong complex with resorcinol, and only a semi-quantitative estimation of  $\log K$  ( $> 20.8$ ) can be determined.

**Table 3.1.** The CIS of Py-2-protons, Py-3-protons and  $ArOH$  referred to  $CDCl_3$  in the presence of various amount of resorcinol

Equivalent of resorcinol	Complexation Induced Shift (CIS)					
	Py-2-protons		Py-3-protons		$ArOH$	
	Hz	$\Delta Hz$	Hz	$\Delta Hz$	Hz	$\Delta Hz$
0.0	1722.163	0.000	1531.387	0.000	1404.654	0.000
0.5	1715.660	-6.503	1561.446	30.059	1435.200	30.546
1.0	1711.278	-10.885	1576.328	44.941	1448.000	43.346
1.5	1708.545	-13.618	1575.684	44.297	1453.067	48.413
2.0	1709.146	-13.017	1576.048	44.661	1452.665	48.011
2.5	1710.801	-11.362	1576.720	45.333	1452.005	47.351
3.0	1708.048	-14.115	1575.358	43.971	1453.280	48.626
4.0	1709.075	-13.088	1576.056	44.669	1452.784	48.130

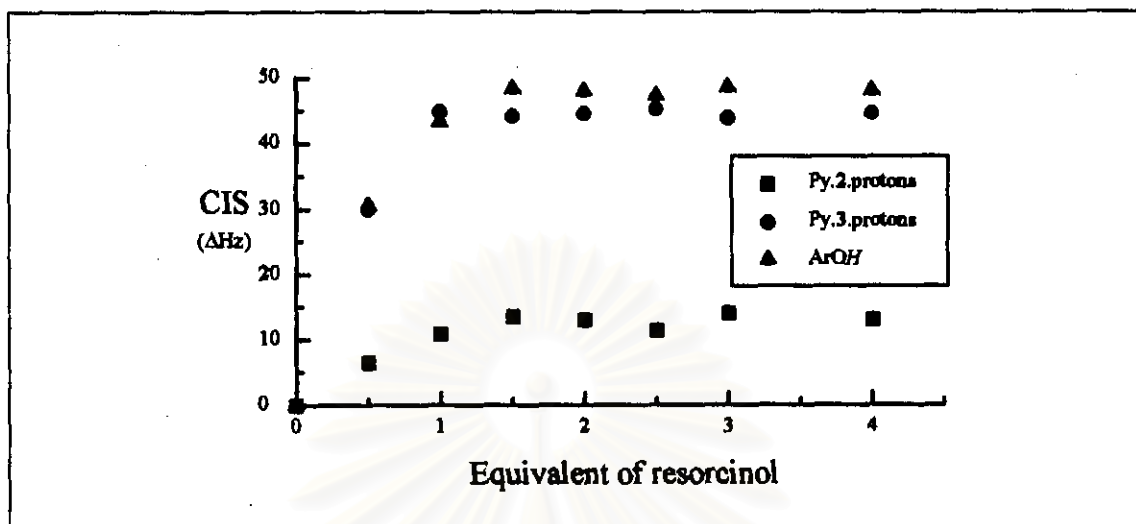


**Figure 3.11.** Plot of CIS of Py-2-protons, Py-3-protons and ArOH against the equivalent of resorcinol.

It must be very interesting to know the solution structure of the 6-resorcinol complex. Thus, NOESY and ROESY experiments for ligand (6) in  $\text{CDCl}_3$  and the mixture of ligand (6) and resorcinol (1:1 ratio) in  $\text{CDCl}_3$  were carried out. Figure 3.12 (a) displays interactions between protons of ligand (6) as deduced from the NOESY and ROESY. From the 2D-NMR results and quantum calculation (using  $\text{MM}^+$  for geometry optimization), the gas phase structure of ligand (6) which showed the preorganized cavity of the ligand (6) was obtained (Figure 3.12 (b)).

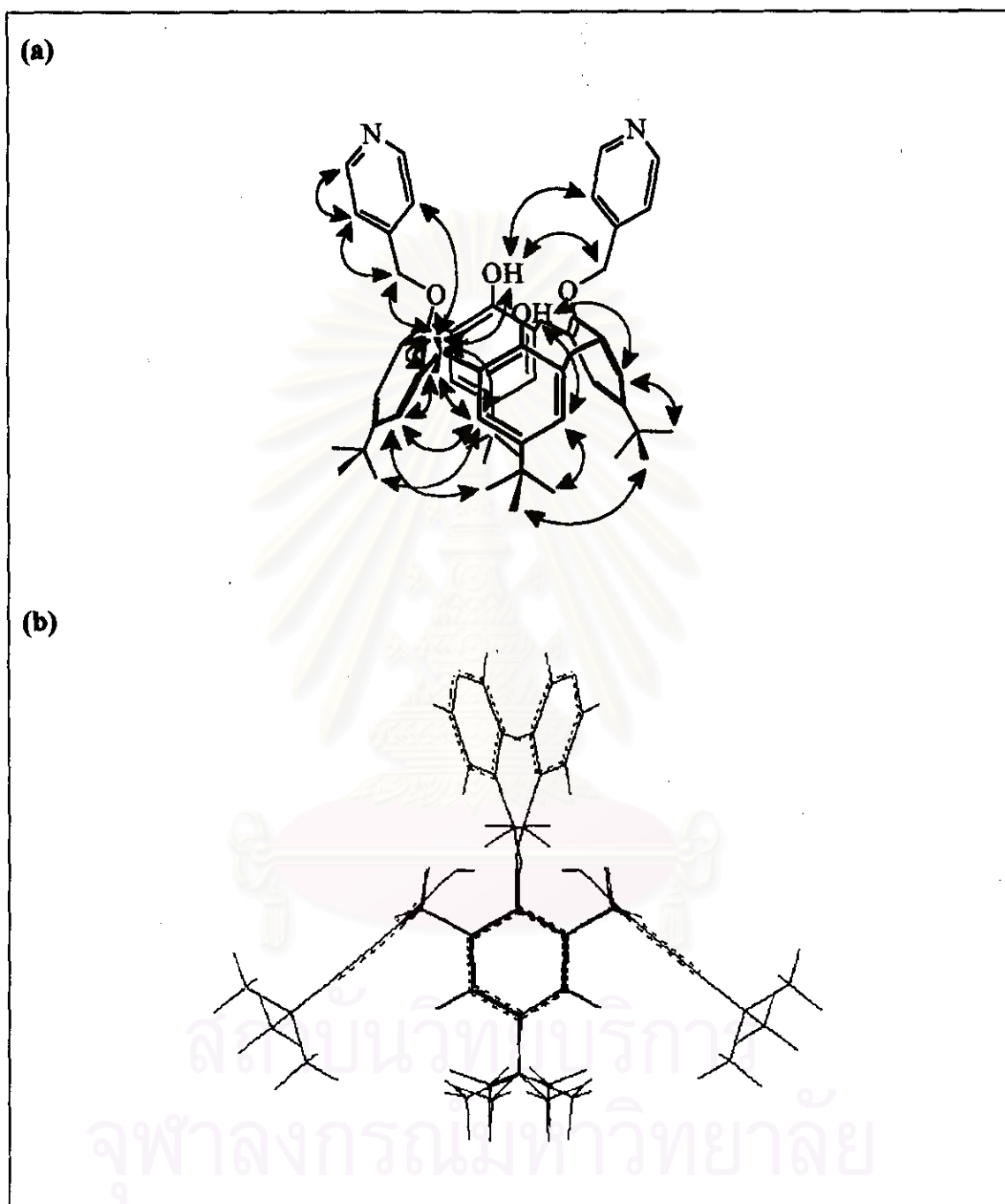


**Figure 3.12.** (a) Interactions between protons of ligand (6) deduced from NOESY and ROESY. ( $\longleftrightarrow$  represents strong interaction and  $\longleftrightarrow$  represents the weak interaction). (b) Gas phase structure of ligand (6) obtained from quantum calculation.



A NOESY of the mixture of ligand (6) and resorcinol in a 1:1 stoichiometry are shown in Figure 3.13. The proton  $H_s$  was found to have a very strong interaction with Py-2-proton while the protons  $H_d$  and  $H_t$  showed very weak interactions with Py-2-proton. In addition, there was no interaction between  $H_s$  and Py-3-proton. The resorcinol molecule must orientate its  $H_s$  into the pyridyl cavity of ligand (6) and pointing  $H_d$  and  $H_t$  outward. This orientation is stabilized by hydrogen bonding interaction between resorcinol-OH and N-pyridyl of ligand (6). A moderate interaction of the proton  $H_d$  with HOArH and ROArH of the calix[4]arene framework has also been observed. Furthermore, the NOESY in Figure 3.13 (b) shows that the proton  $H_s$  has a moderate interaction with *t*-butyl protons (b) of the ArOH rings. Figure 3.14 summarizes the interactions of protons in a 1:1 mixture of ligand (6) and resorcinol. These interactions imply that a resorcinol molecule must also be included into the hydrophobic upper rim cavity of another calix[4]arene unit of ligand (6). The results are consistent with the upfield shift of Py-2-proton which stems from the diamagnetic anisotropy of the neighboring ring current (from aromatic wall of calix [4]arene or resorcinol). The possible solution structure of 6-resorcinol is proposed in Figure 3.15.

สถาบันวิทยบริการ  
จุฬาลงกรณ์มหาวิทยาลัย

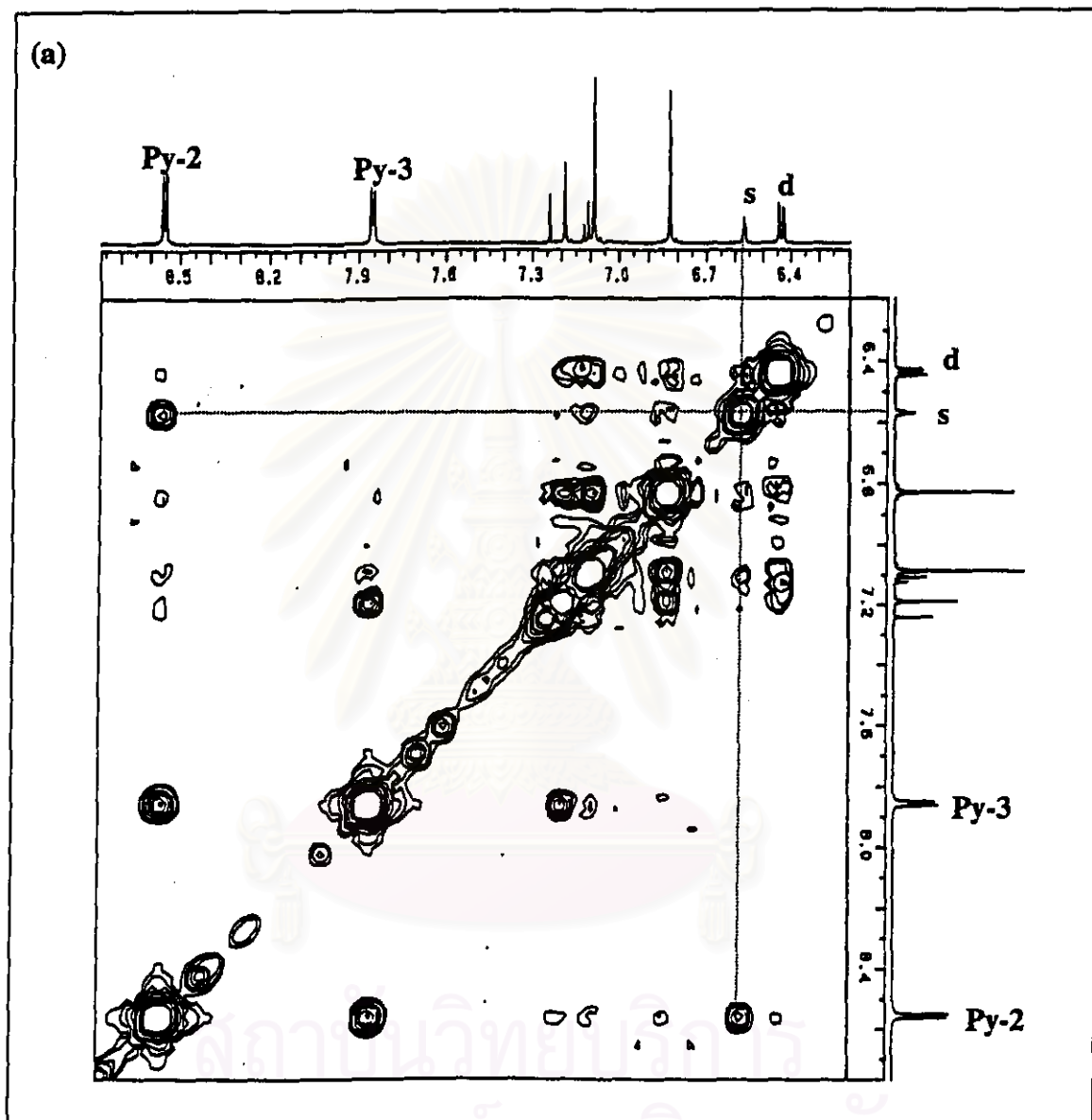


**Figure 3.13.** NOESY of a 1:1 mixture of ligand (6) and resorcinol in the range of (a) 6.2-8.7 and (b) 0.5-7.5 ppm.

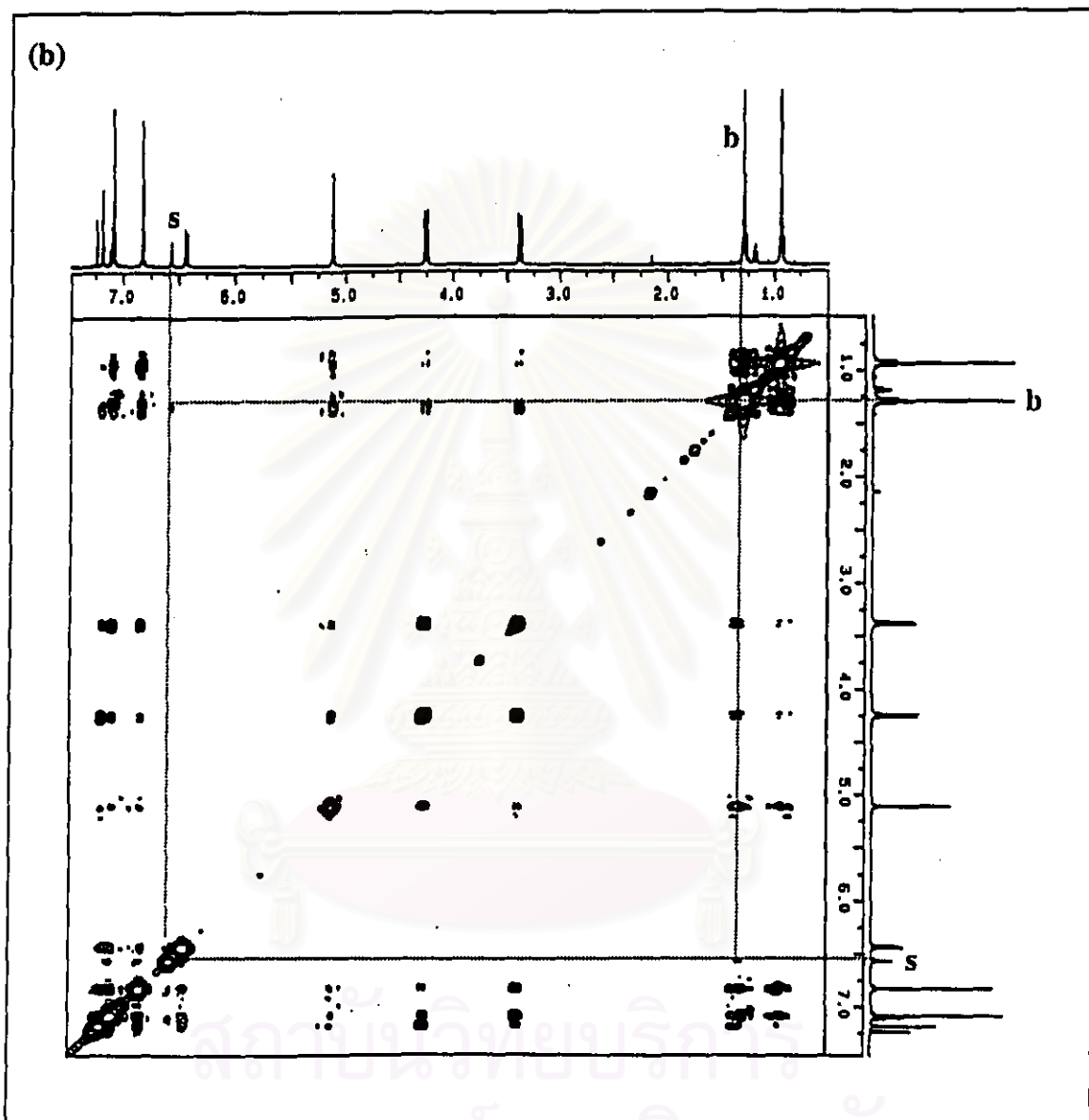
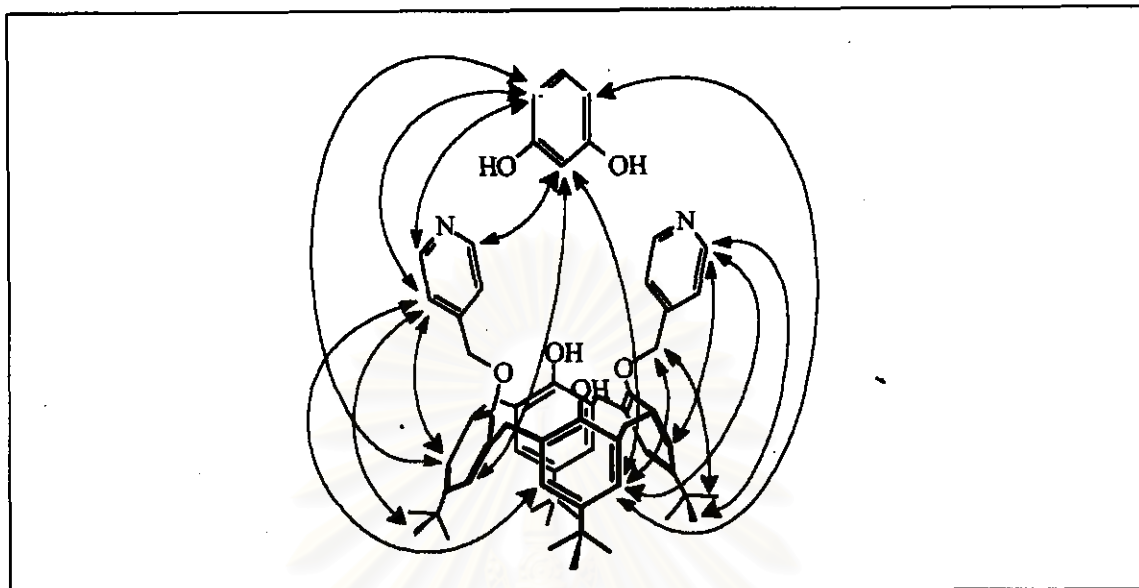


Figure 3.13. *continue.*



**Figure 3.14.** The interaction in a mixture of resorcinol and ligand (**6**) deduced from NOESY and ROESY experiments.

The receptor molecules should be linked together in a head to tail fashion using the resorcinol molecules as linkage (Figure 3.15) resembling the silver bridge in self-assembly of tetracyanocalix[4]arene<sup>42</sup>. The hydrophobic/hydrophilic and hydrogen bonding interactions of the host and the guest can thus be accounted for the exceptionally high stability of the **6**-resorcinol complex.

สถาบันวิทยบริการ  
จุฬาลงกรณ์มหาวิทยาลัย

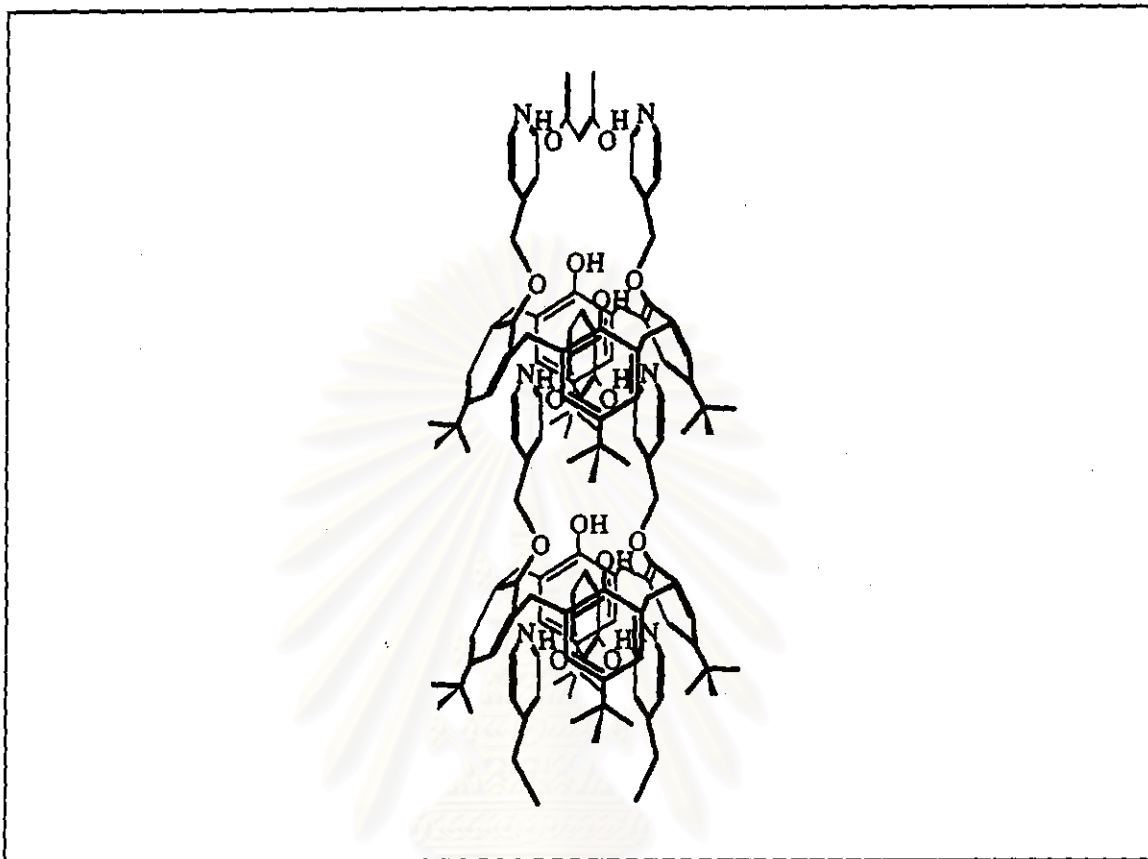


**Figure 3.15.** The possible solution structure of the 6-resorcinol complex.

The complexation of ligand (6) and resorcinol was also studied in methanol- $d_4$  and DMSO- $d_6$ . Unfortunately, the results show that ligand (6) does not complex resorcinol in both solvents<sup>43-44</sup>. In deuterated methanol, the complexation of ligand (6) and resorcinol may be disrupted and replaced by the stronger hydrogen bonding interaction of methanol towards ligand (6) and resorcinol because the hydroxy group of methanol can act as both hydrogen bond donors and hydrogen bond acceptors. Either hydrogen bond donor character of O-atom or the presence of  $H_2O$  in deuterated DMSO is also accounted for the absence of hydrogen bonding interaction between ligand (6) and resorcinol.

### 3.2.2.1.2 Complexation Studies of 1,2-Dihydroxybenzene (Catechol)

A typical  $^1\text{H-NMR}$  spectrum of a mixture of catechol and ligand (6) is shown in Figure 3.16. The spectrum shows a doublet of doublet signal at 3.34 and 4.22 ppm signifying the cone conformation of the calix[4]arene framework. Upon addition of catechol, all protons on ligand (6) except Py-2-proton shifted downfield. The CIS is illustrated in Figure 3.17.

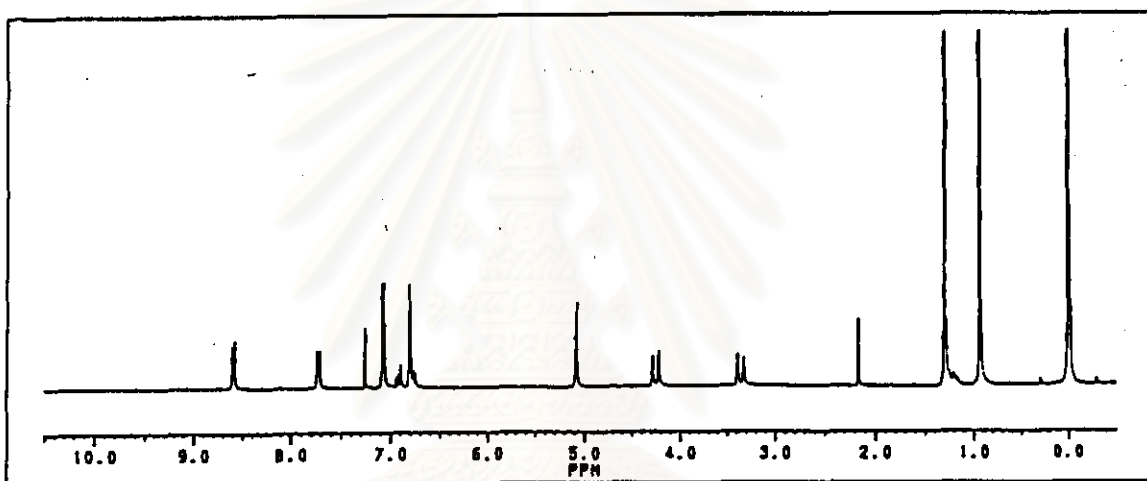
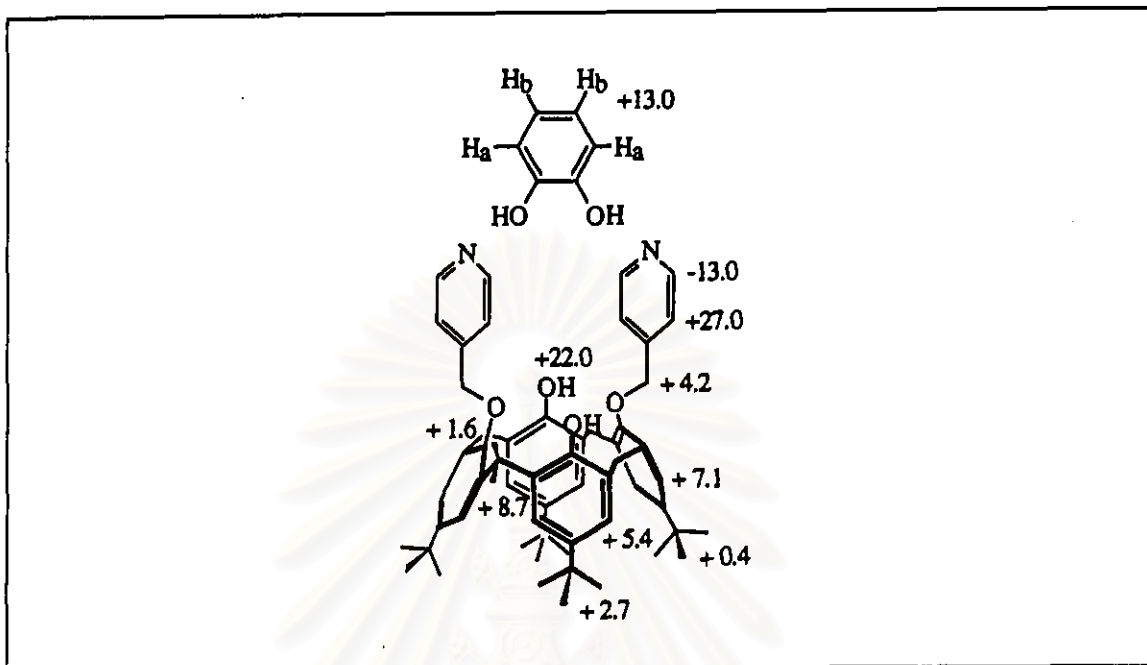


Figure 3.16.  $^1\text{H-NMR}$  spectrum of a 1:1 mixture of catechol and ligand (6).

สถาบันวิทยบริการ  
จุฬาลงกรณ์มหาวิทยาลัย



**Figure 3.17.** The CIS ( $\Delta\delta$  (Hz)) of protons on ligand (6) when complexing with catechol (at 1:4 ratio).

Interestingly, further addition of up to 10 equivalents of catechol produced significant shifts of all protons of ligand (6) (Table 3.2, Figure 3.18) except Py-3-proton. Only CIS of Py-3-proton suggests that the interaction between the aromatic protons of catechol and the aromatic protons of ligand (6) is a 4:1 stoichiometry. Therefore, the stability constant cannot be calculated using our curve-fitting program. In addition, it should be noted that the inclusion of catechol by ligand (6) could be occurred in spite of the low solubility of catechol (>10 equivalents of catechol was added). The hydrogen bonding interaction between catechol and ligand (6) must be stronger than that between catechol itself.

**Table 3.2.** The CIS of Py-2-protons, Py-3-protons and ArOH in the presence of various amount of catechol

Equivalent of catechol	Complexation Induced Shift					
	Py-2-protons		Py-3-protons		ArOH	
	Hz	$\Delta$ Hz	Hz	$\Delta$ Hz	Hz	$\Delta$ Hz
0.0	1723.749	0.000	1533.145	0.000	1401.111	0.000
0.2	1723.239	-0.511	1535.919	2.774	1402.306	1.195
0.4	1722.470	-1.280	1538.853	5.708	1404.079	2.968
0.6	1721.564	-2.186	1541.658	8.513	1405.494	4.383
0.8	1720.396	-3.353	1544.057	10.912	1407.401	6.290
1.0	1719.892	-3.857	1546.240	13.095	1408.406	7.295
1.2	1718.838	-4.912	1548.611	15.466	1410.136	9.025
1.5	1717.256	-6.493	1550.423	17.278	1412.401	11.290
1.8	1715.877	-7.873	1552.311	19.166	1414.168	13.057
2.0	1715.889	-7.860	1552.975	19.830	1414.323	13.212
2.2	1714.693	-9.057	1553.787	20.642	1414.986	13.875
2.5	1713.973	-9.776	1555.144	21.999	1417.118	16.007
2.8	1712.616	-11.133	1555.785	22.640	1418.679	17.568
3.0	1711.956	-11.793	1556.178	23.033	1419.658	18.574
3.2	1712.196	-11.554	1556.415	23.270	1419.403	18.292
4.0	1709.628	-14.121	1557.950	24.805	1423.408	22.297



Attempts to elucidate the solution structure of **6**-catechol have been carried out by NOESY and ROESY experiments. NOESY of the mixture of ligand (**6**) and catechol in a 1:2 ratio and a 1:4 ratio are depicted in Figure 3.19 (a) and 3.19 (b), respectively. It is found that the proton of catechol has a strong interaction with Py-2-proton and a weak interaction with Py-3-proton, Ar-OCH<sub>2</sub>-Py and Ar-CH<sub>A</sub>H<sub>B</sub>-Ar. The interactions among protons of **6**-catechol deduced from NOESY are summarized in Figure 3.20.



สถาบันวิทยบริการ  
จุฬาลงกรณ์มหาวิทยาลัย

Table 3.2. *continue*

Equivalent of catechol	Complexation Induced Shift					
	Py-2-protons		Py-3-protons		ArOH	
	Hz	$\Delta$ Hz	Hz	$\Delta$ Hz	Hz	$\Delta$ Hz
5.0	1706.202	-17.547	1558.453	25.308	1428.141	27.030
6.0	1704.021	-19.726	1558.476	25.331	1431.392	30.281
7.0	1702.356	-21.393	1558.236	25.091	1433.762	32.651
8.0	1700.063	-23.687	1557.754	24.609	1437.200	36.089
9.0	1698.220	-25.529	1557.019	23.874	1439.348	38.237
10.0	1697.570	-26.180	1556.717	23.572	1440.050	38.939

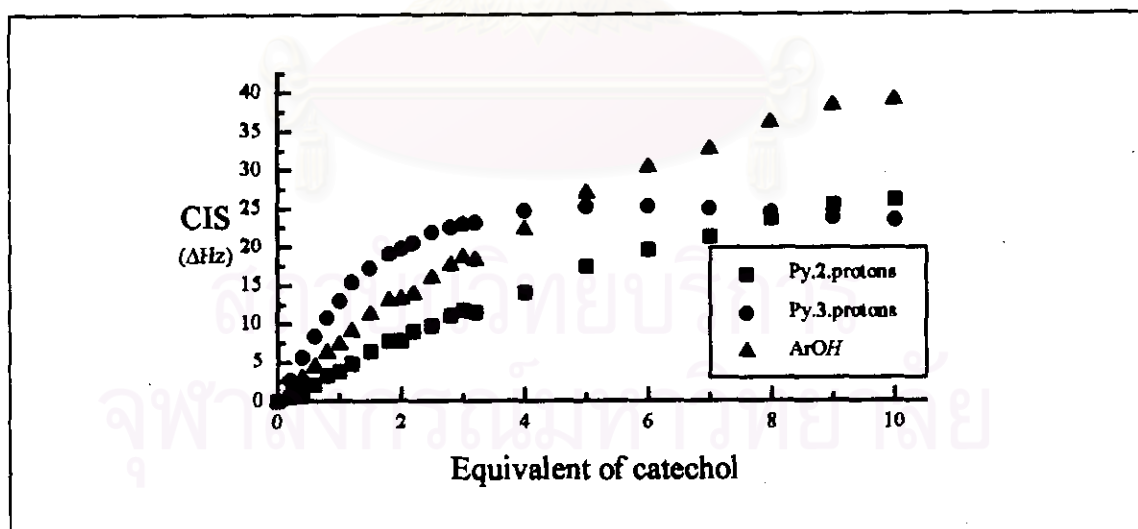


Figure 3.18. Plot of CIS of Py-2-protons, Py-3-protons and ArOH against the equivalent of catechol.

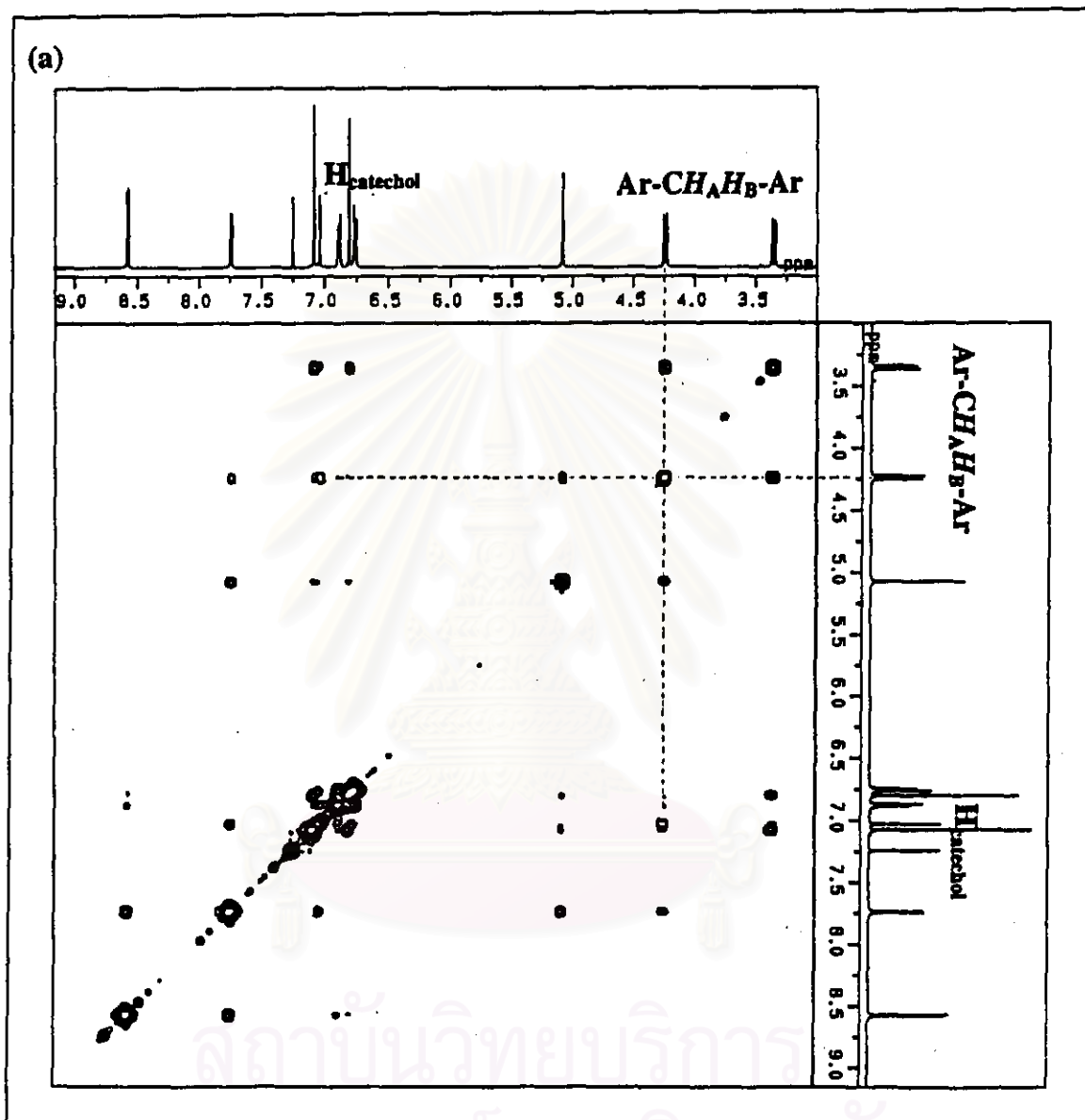


Figure 3.19. NOESY of a mixture of catechol and ligand (6) (a) 2:1 and (b) 4:1 stoichiometry.

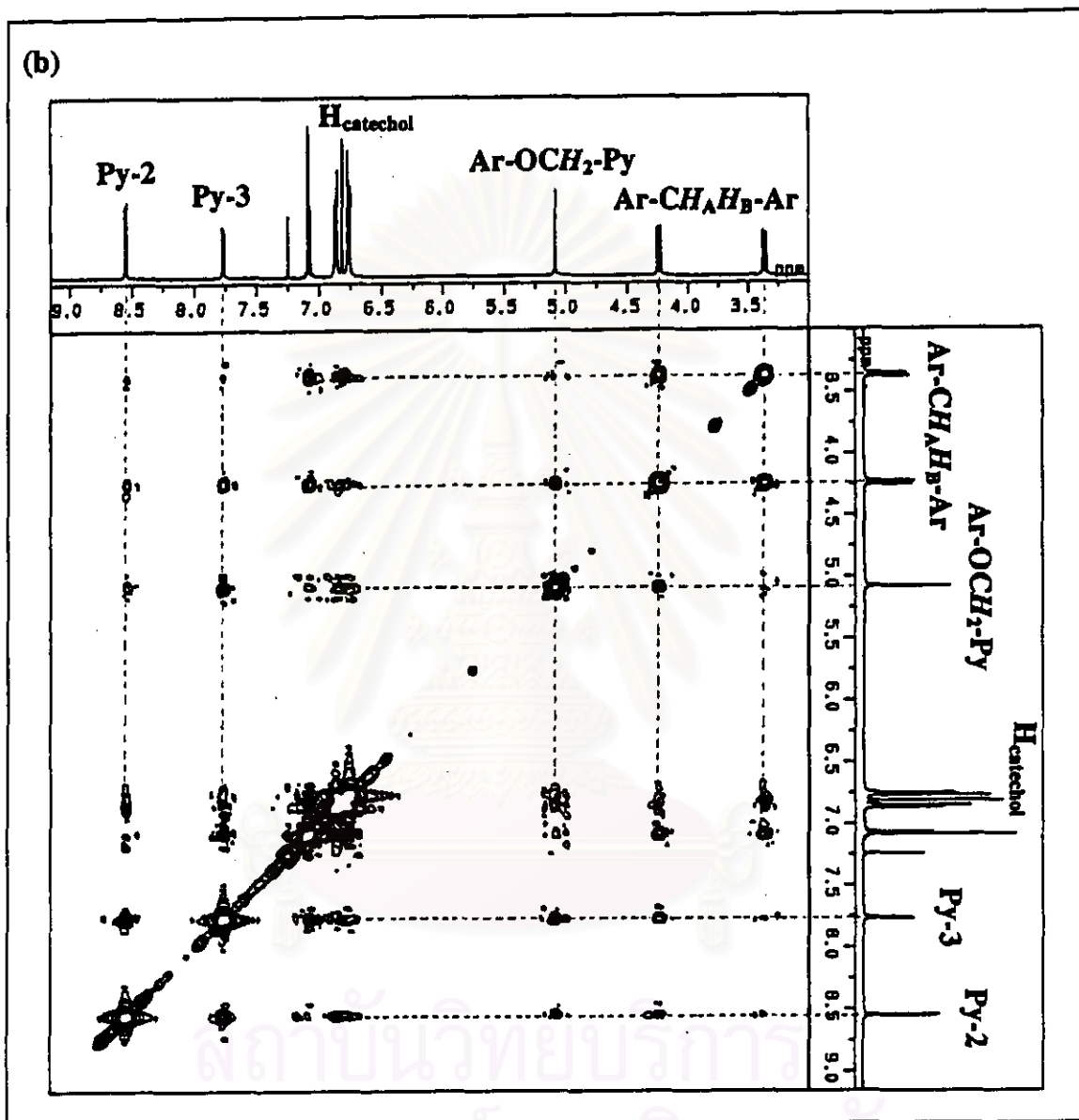
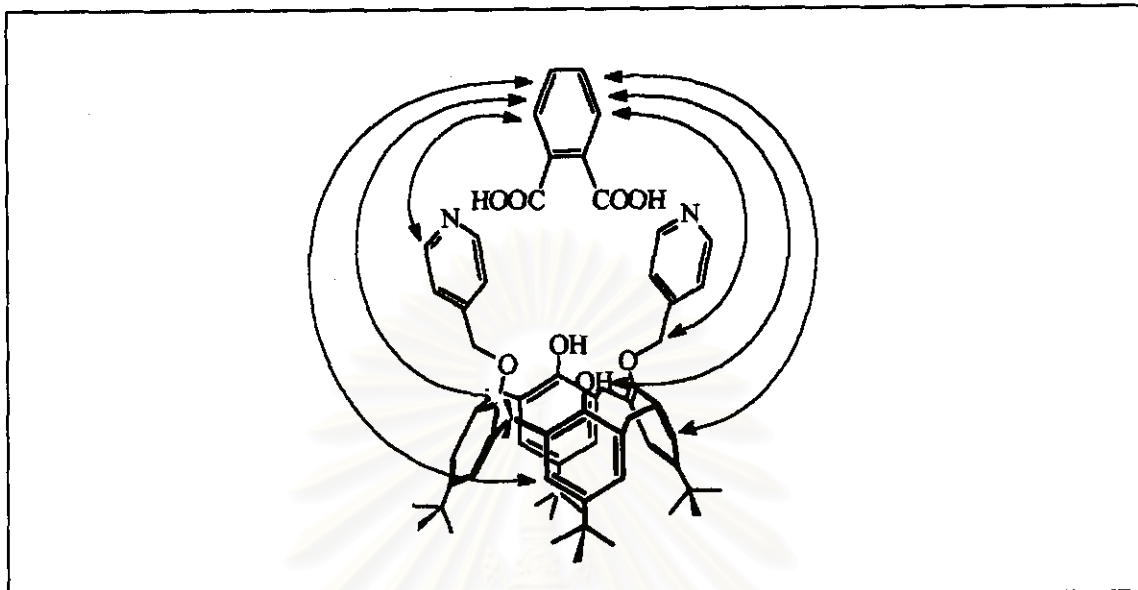


Figure 3.19. *Continue.*



**Figure 3.20.** The interactions of protons in 6-catechol deduced from NOESY.

In addition, an NMR study on the interaction of pyridine towards catechol was also performed. The result suggests that catechol forms a complex with pyridine in a 1:2 fashion. Considering our ligand (**6**) containing two pyridyl groups, the formation of a 1:4 complex is quite possible and also corresponds to the titration results. Two possible solution structures of 6-catechol which represent possible 1:4 complexes are thus proposed in a polymeric fashion (Figure 3.21). Both structures account for hydrogen bonding interactions at the N-pyridyl and the OH-phenoxy of the calix[4]arene moiety, and the unlimited shifting of the proton signals. Structures (a) and (b) are also consistent with the upfield shift of Py-2-proton which is attributed to magnetic anisotropy.

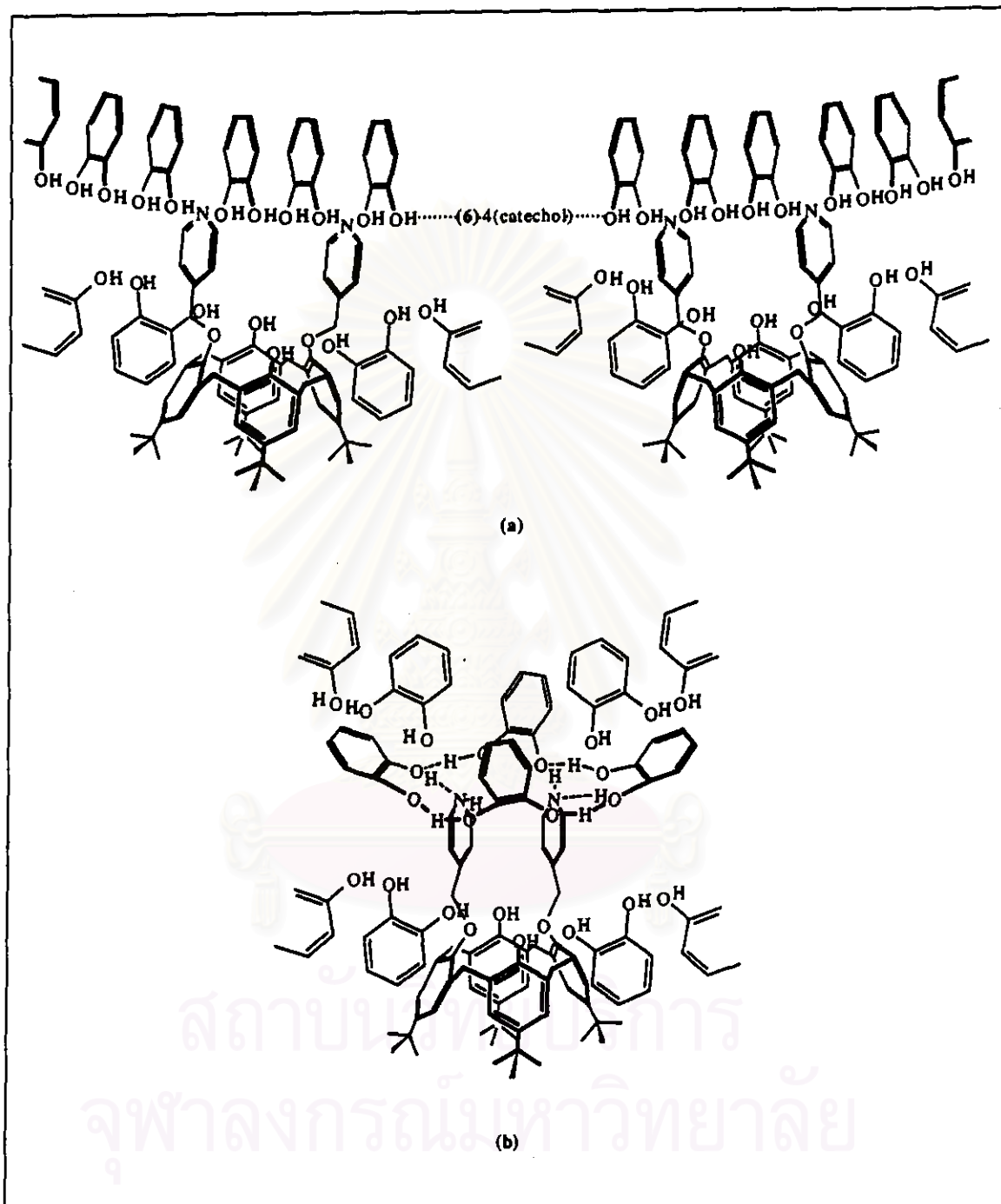


Figure 3.21. The possible structures of the 6-catechol complex.

Although the stability constant of the 6-catechol complex cannot be determined, the comparative binding ability of catechol and resorcinol can be estimated. Addition of various stoichiometry of 6-catechol in  $\text{CDCl}_3$  into the same ratio of resorcinol resulted in the shifting of proton signals which was similar to the shifting in 6-resorcinol (Table 3.3). The result signifies that catechol in 6-catechol has been replaced by resorcinol. Therefore, ligand (6) forms a more stable complex with resorcinol.

**Table 3.3.** Complexation Induced Shift of proton signals for 6-catechol, 6-resorcinol and the result from competitive studies

Signals	Complexation Induced Shift ( $\Delta\delta$ (Hz))		
	6-catechol	competitive studies	6-resorcinol
Py-2-proton	- 13.0	- 11.0	- 10.0
Py-3-proton	+27.0	+46.0	+45.0
HOArH	+ 5.4	+ 5.6	+ 5.6
ROArH	+ 7.1	+ 5.4	+11.0
ArOH	+22.0	+46.0	+48.0
Ar-OCH <sub>2</sub> -Py	+ 4.2	+12.7	+12.0
ArCH <sub>A</sub> H <sub>B</sub> Ar	+ 1.6, +8.7	+ 4.1, +13.2	+ 4.6, +13.0
HOAr- <i>t</i> -C <sub>4</sub> H <sub>9</sub>	+ 2.7	+ 1.5	+ 1.8
ROAr- <i>t</i> -C <sub>4</sub> H <sub>9</sub>	+ 0.4	+ 3.8	+ 4.4

In case of hydroquinone, no CIS of signals in  $^1\text{H-NMR}$  spectra is observed indicating that no complex of 6-hydroquinone has occurred. This result may stem from the unmatching size and hydrogen bonding direction between host and guest molecules, *vide infra*.

### 3.2.2.2 Complexation Studies of Benzene-Dicarboxylic Acids

Ligand (6) has been studied its ability to form complexes with dicarboxylic acids such as phthalic acid, isophthalic acid and terephthalic acid by  $^1\text{H-NMR}$  titration. It was found that isophthalic acid and terephthalic acid did not form complexes with ligand (6)<sup>45</sup>, *vide supra*. Only phthalic acid was found to dissolve into a  $\text{CDCl}_3$  solution of ligand (6) and the complex formation constant could be estimated by  $^1\text{H-NMR}$  spectroscopy.

#### 3.2.2.2.1 Complexation Studies of Phthalic Acid

$^1\text{H-NMR}$  studies were carried out by direct addition of the acid as solid into  $\text{CDCl}_3$  solutions of ligand (6). A typical  $^1\text{H-NMR}$  spectrum of the mixture is displayed in Figure 3.22. The calix[4]arene compartment is still in a cone conformation judging by the presence of a doublet of doublet signals at 3.40 and 4.22 ppm. Upon increasing the amount of phthalic acid, all protons on ligand (6) except  $\text{ArOH}$  shifted downfield. The CIS of protons is shown in Figure 3.23.

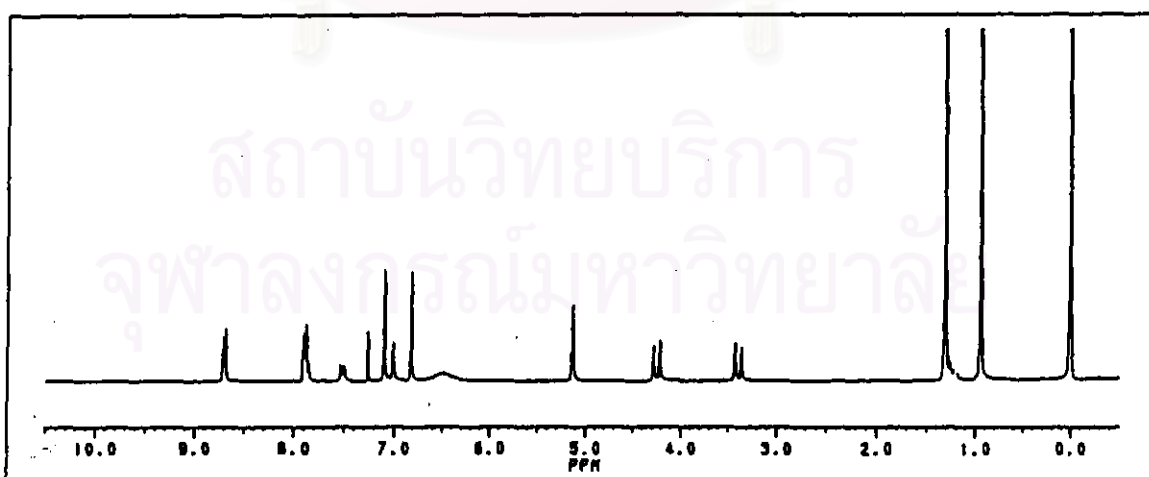
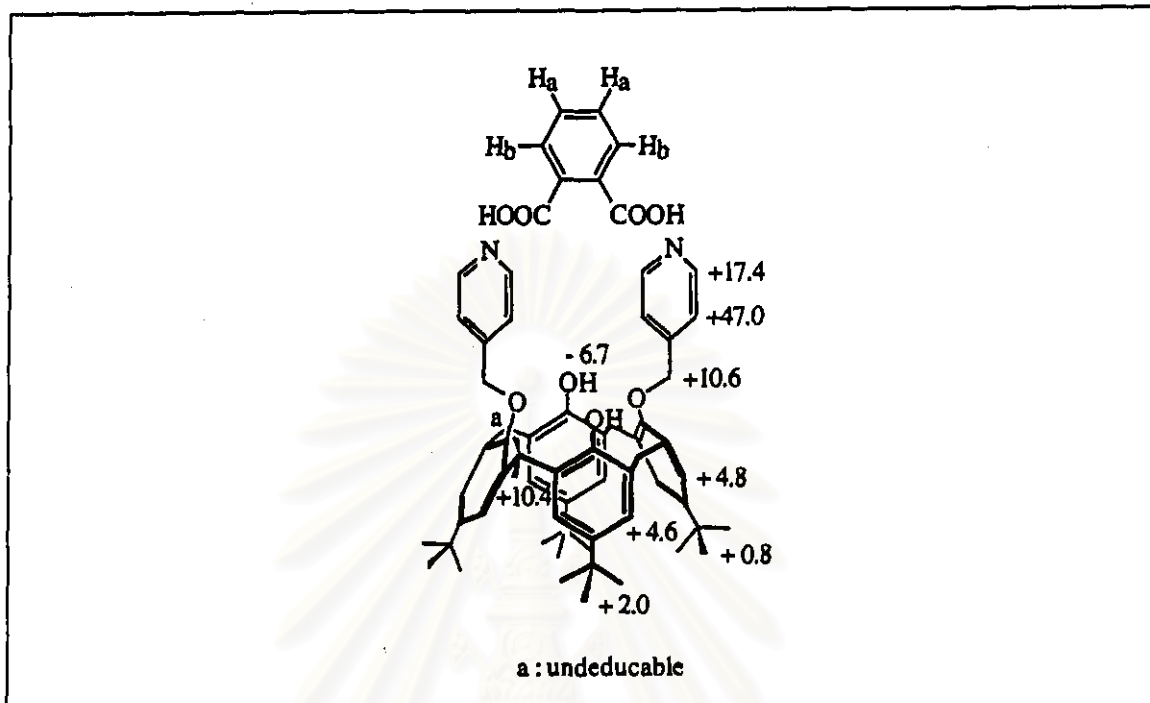


Figure 3.22.  $^1\text{H-NMR}$  spectrum of a mixture of ligand (6) and phthalic acid.





**Figure 3.23.** The CIS ( $\Delta\delta$  (Hz)) of all protons on ligand (6) when complexing phthalic acid.

Interestingly, Py-2-proton which was closer to the center of hydrogen bonding shifted less downfield than Py-3-proton did. Py-2-proton, Py-3-proton and ArOH were used for estimating a stability constant. The titration results shown in Table 3.4 and Figure 3.24 suggest a 1:1 stoichiometry of the 6-phthalic acid complex. The complex formation constant of 6-phthalic acid was estimated to be  $\log K = 5.41$ .

**Table 3.4.** The CIS of Py-2-protons, Py-3-protons and ArOH upon addition of various amount of phthalic acid into ligand (6)

Equivalent of phthalic acid.	Complexation Induced Shift					
	Py-2-protons		Py-3-protons		ArOH	
	Hz	$\Delta$ Hz	Hz	$\Delta$ Hz	Hz	$\Delta$ Hz
0.0	1722.370	0.000	1531.031	0.000	1402.244	0.000
0.5	1734.420	12.050	1563.537	32.506	1397.104	-5.140
1.0	1739.719	17.349	1577.608	46.577	1395.806	-6.438
1.5	1739.267	16.897	1576.899	45.868	1395.603	-6.641
2.0	1739.828	17.458	1578.380	47.349	1395.880	-6.364
2.5	1739.887	17.517	1578.388	47.357	1395.844	-6.400
3.0	1739.796	17.426	1577.767	46.736	1395.105	-7.139
4.0	1739.832	17.462	1578.486	47.455	1395.652	-6.592

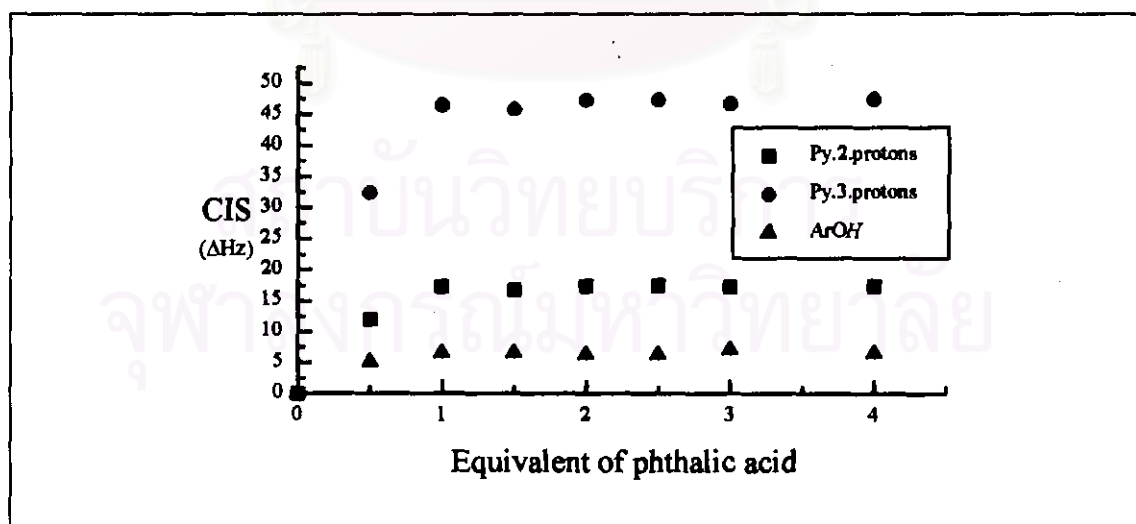


**Figure 3.24.** Plot of the CIS of Py-2-protons, Py-3-protons and ArOH against the equivalent of phthalic acid.

NOESY and ROESY experiments of the 1:1 mixture of ligand (6) and phthalic acid were performed in  $\text{CDCl}_3$  and the spectra are depicted in Figure 3.25 and 3.26, respectively.

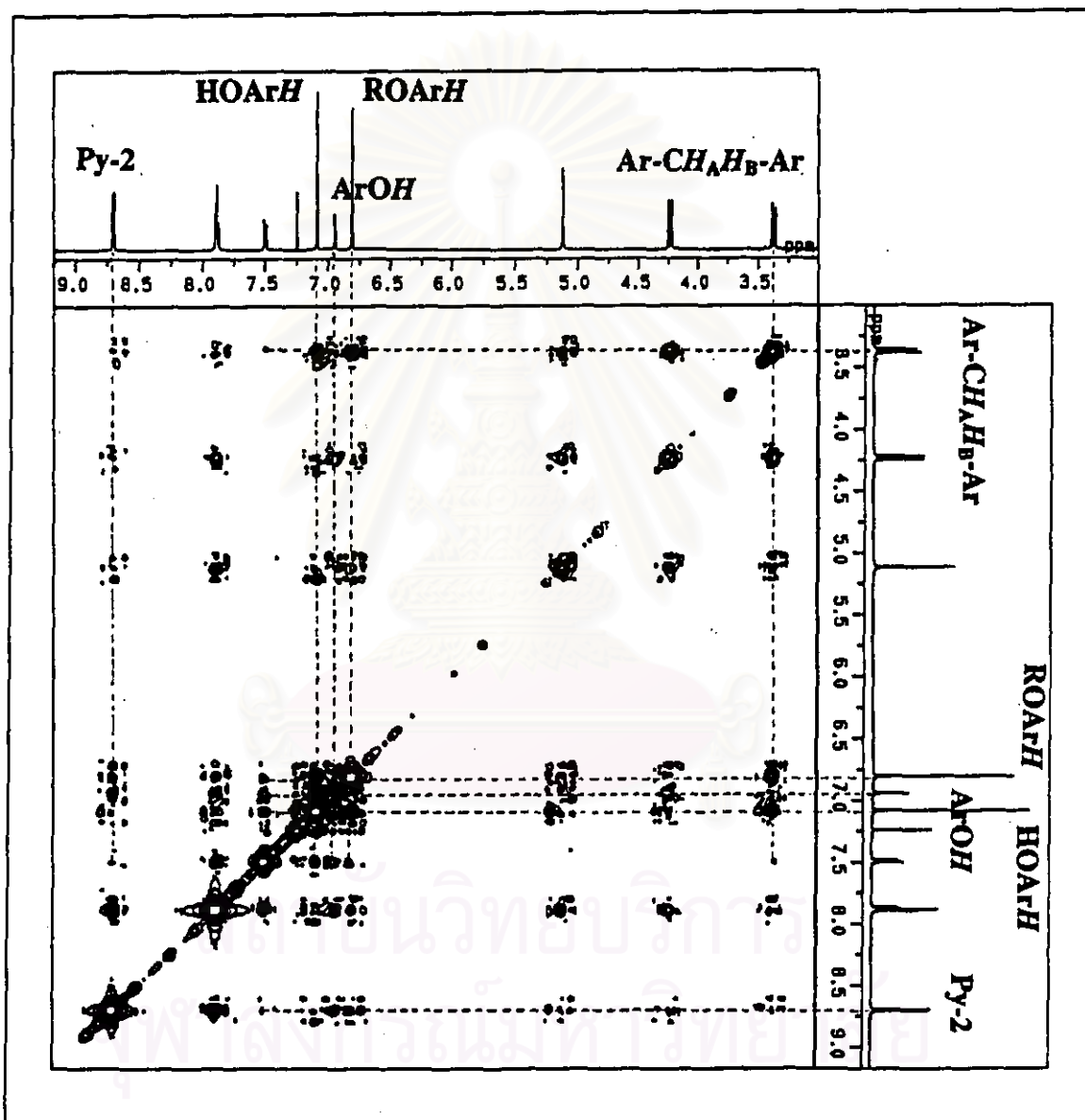


Figure 3.25. NOESY of a 1:1 mixture of ligand (6) and phthalic acid.

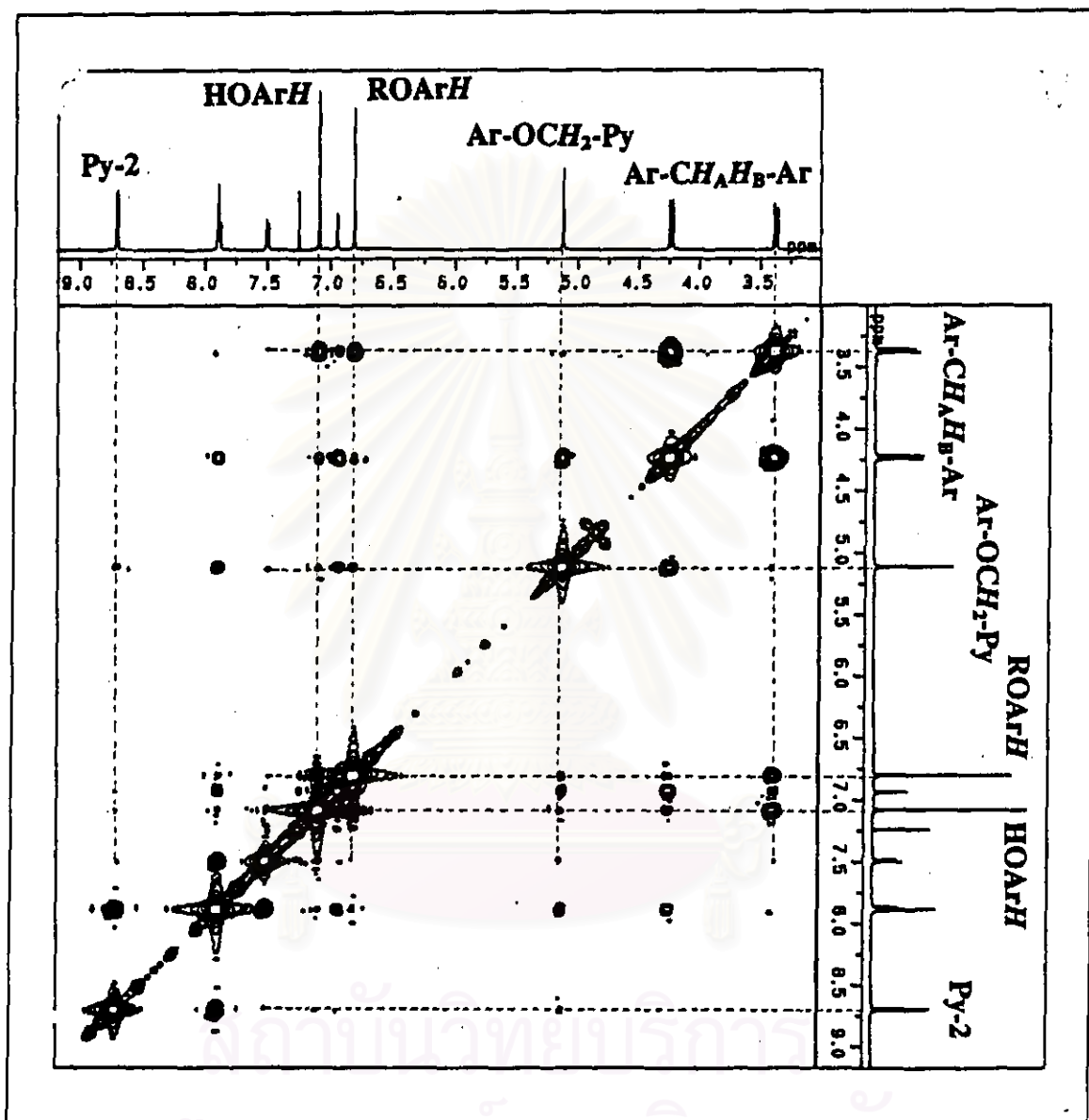
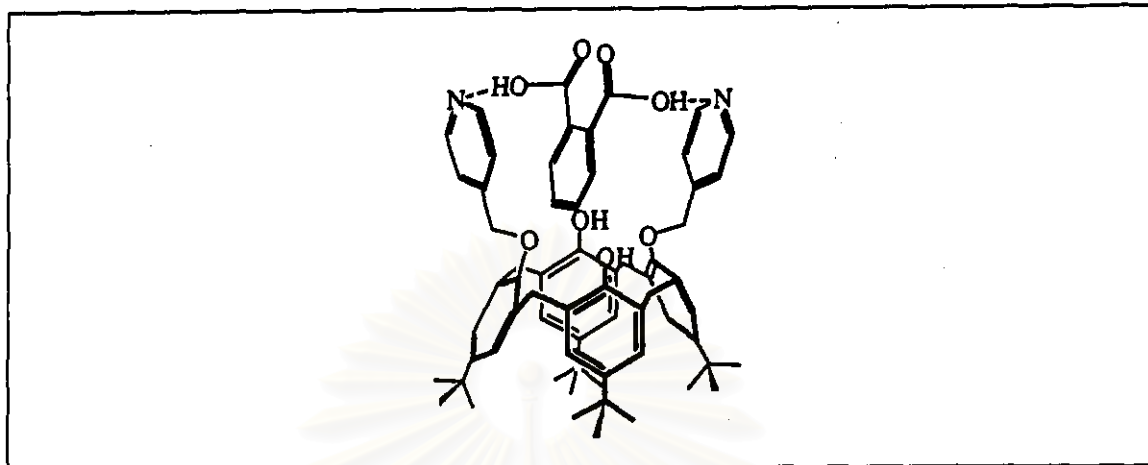


Figure 3.26. ROESY of a 1:1 mixture of ligand (6) and phthalic acid.



**Figure 3.28.** Possible solution structure of the 6-phthalic acid complex.

The competitive study of 6-phthalic acid and catechol has also been carried out by  $^1\text{H-NMR}$  titration in a similar manner to the 6-resorcinol case. The results are collected in Table 3.5. Obviously, the CIS of protons of the product is very similar to that of 6-phthalic acid. This implies that ligand (6) forms a more stable complex with phthalic acid<sup>49</sup>.

สถาบันวิทยบริการ  
จุฬาลงกรณ์มหาวิทยาลัย

One of the aromatic signals on phthalic acid is superimposed on the signal of Py-3-proton. Therefore, some interactions related to these protons cannot be distinguished. However, strong interactions of protons on phthalic acid towards *ArOH* and *Ar-OCH<sub>2</sub>-Py* of ligand (**6**) as well as weak interactions towards Py-2-proton, *ArCH<sub>A</sub>H<sub>B</sub>Ar* and *HOArH* can be observed unambiguously (Figure 3.27). The results imply that phthalic acid reside within the cavity of ligand (**6**) close to *ArOH* and *Ar-OCH<sub>2</sub>-Py*. The possible solution structure of the **6**·phthalic acid complex can thus be drawn as shown in Figure 3.28.

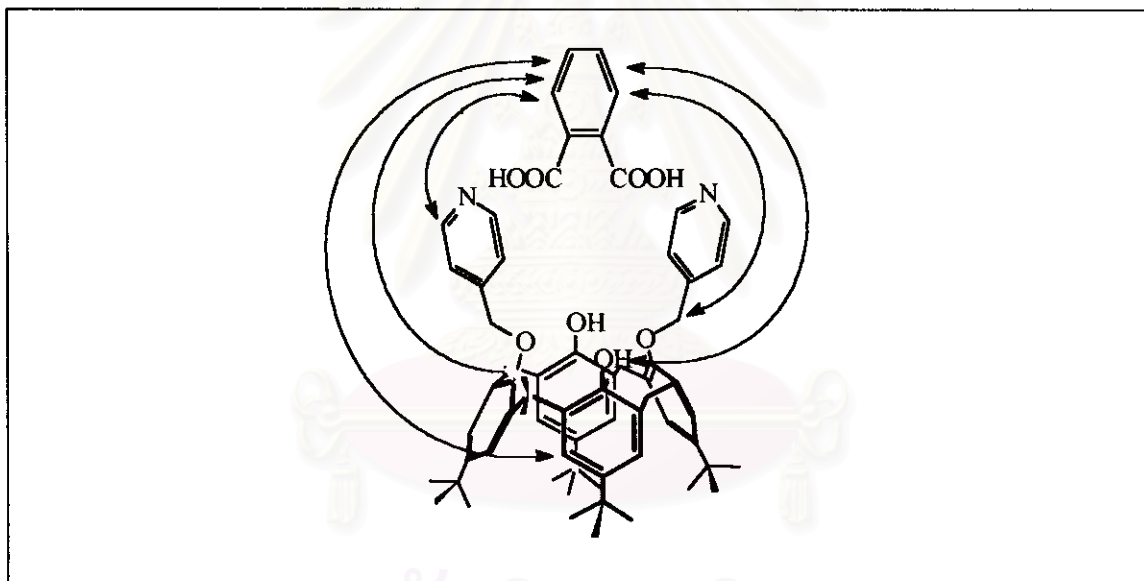


**Figure 3.27.** The interactions of protons in a 1:1 mixture of ligand (**6**) and phthalic acid deduced from NOESY and ROESY.

The structure agrees with the fact that *ArOH* shifted upfield due to the anisotropic effect of phthalic ring current. Besides hydrogen bonding, the stability of the complex may be ascribed to  $\pi$ - $\pi$  stacking interactions<sup>46-48</sup> of ligand (**6**) and phthalic acid.

**Table 3.5.** Complexation Induced Shift of proton signals for 6-catechol, 6-phthalic acid and the result from competitive studies

Signals	Complexation Induced Shift ( $\Delta\delta$ (Hz))		
	6-catechol	Competitive studies	6-phthalic acid
Py-2-proton	- 13.0	+15.0	+17.4
Py-3-proton	+27.0	+45.0	+47.0
HOArH	+ 5.4	+ 4.7	+ 4.6
ROArH	+ 7.1	+ 5.5	+ 4.8
ArOH	+22.0	- 9.3	- 6.7
Ar-OCH <sub>2</sub> -Py	+ 4.2	+10.7	+10.6
ArCH <sub>A</sub> H <sub>B</sub> Ar	+ 1.6, +8.7	- 1.3, +18.0	<sup>a</sup> , +10.4
HOAr- <i>t</i> -C <sub>4</sub> H <sub>9</sub>	+ 2.7	+ 1.8	+ 2.0
ROAr- <i>t</i> -C <sub>4</sub> H <sub>9</sub>	+ 0.4	+ 1.2	+ 0.8

<sup>a</sup> undeducable

### 3.2.2.3 Matching between Cavity Size of Ligand (6) and Size of the Guests Based on Theoretical Calculation

The structure of ligand (6) calculated by molecular mechanic method (MM<sup>+</sup>) was found to be a preorganized structure possessing a N<sub>Py</sub>-N<sub>Py</sub> distance of 6.34 Å. Therefore, ligand (6) can accommodate a guest which is smaller than 6.34 Å. The structures of dicarboxylic acids and benzene dialcohols used in the complexation studies of ligand (6) were also calculated by the same method. The results are depicted in Table 3.6.

**Table 3.6.** Structures and  $H_A-H_B$  distances of benzene-dialcohols and benzene-dicarboxylic acids

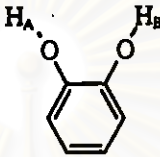
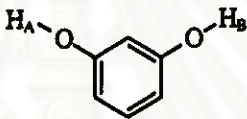
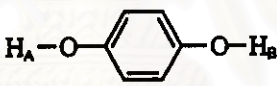
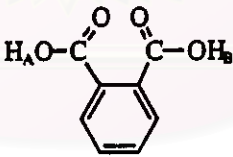
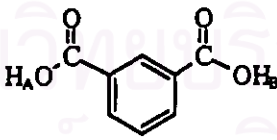
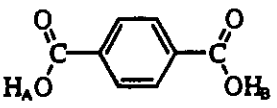
Name	Structure	$H_A-H_B$ distances (Å)
Catechol		3.29
Resorcinol		4.58
Hydroquinone		6.39
Phthalic acid		5.82
Isophthalic acid		8.68
Terephthalic acid		9.13



Table 3.6 shows that only catechol, resorcinol and phthalic acid are suitable to be included into the cavity of ligand (6) to form complexes. This is pertinent to the results from  $^1\text{H-NMR}$  studies. Only phthalic acid has a suitable geometry and can use its hydroxy groups to form hydrogen bonding with N-pyridyl of ligand (6) and simultaneously be included into the pyridyl cavity of ligand (6). The geometry of catechol and resorcinol are obviously too constrained to perform such task. Catechol can interact with ligand (6) in a 1:4 fashion. This may stem from the versatility of catechol to form either intramolecular or intermolecular hydrogen bonding. Such properties may lead to the formation of homonuclear hydrogen bonding (catechol-catechol) and heteronuclear hydrogen bonding (catechol-ligand (6)). When resorcinol interacts with N-pyridyl of ligand (6), its eclipse orientation (compared to the orientation of the phenyl ring in calix[4]arene) is appropriate for its inclusion into a upper rim cavity of calix[4]arene. Combination of hydrogen bonding and hydrophobic/hydrophilic interactions thus resulted in the exceptionally high stability of the 6-resorcinol complex in  $\text{CDCl}_3$ .

สถาบันวิทยบริการ  
จุฬาลงกรณ์มหาวิทยาลัย